CHAPTER 4

MULTI-OBJECTIVE OPTIMIZATION OF PROCESS PARAMETERS FOR REDUCTION OF ENERGY CONSUMPTION AND CARBON EMISSIONS

This chapter presents the experimental investigations to analyze and reduce the energy consumption and carbon emissions, maintaining the required surface quality, for milling process under dry and wet conditions.

4.1 INTRODUCTION

Traditionally, production rate and surface roughness have been considered as important objectives for any manufacturing process (Camposeco-Negrete, 2013; Gaitonde et al., 2012; Jawahir and Balaji, 2000; Samanta and Nataraj, 2008; Sivasakthivel et al., 2012). This is because the surface roughness is a widely used index of product quality in terms of various parameters such as aesthetics, corrosion resistance, subsequent processing advantages, tribological considerations, fatigue life improvement, precision fit of critical mating surfaces, etc. (Kant and Sangwan, 2014); and production rate is of more interest to industries for economic reasons. The productivity and capability of a machine tool to produce the desired surface finish depend on machining parameters, cutting phenomenon, workpiece properties, cutting tool properties, etc. (Yi et al., 2015). In recent years, because of the increasing importance to sustainability; energy consumption and carbon emissions of machining activities have gained more importance. Many factors like increasing cost, sustainable development, energy security, and political compulsions force nations and industry to strive for energy and carbon efficiencies. High carbon emissions from machining processes put an additional financial burden on the manufacturing organizations due to strict carbon policies. As a consequence, manufacturing industries are

motivated to consider energy consumption and carbon emission issues along with conventional production objectives such as quality and productivity. The energy consumption and carbon emissions caused by CNC machine tools vary with cutting parameters (Li et al., 2013). Hence, the overall performance of the machining processes can be improved in terms of economy and environmental impacts by understanding the relationship among the process responses (surface roughness, energy consumption, MRR, carbon emissions, tool life, etc.) and cutting parameters. The optimization of the energy consumption, carbon emissions and surface roughness will be a contribution towards achieving the sustainable production goals.

Various modelling and optimization methodologies have been developed, used, and expanded by researchers to determine optimum operating conditions for cost effective and eco-friendly machining processes. To produce high-quality products with minimum cost and time, it is essential to optimize the machining parameters. Machining is a complex system consisting large number of variables and multiple contradictory objectives. Improvement in one process response often demands for sacrifice in some other response. Multi-objective optimization is an effective technique to identify trade-off between multiple process responses. A number of studies used optimization techniques to improve one or more of machining process objectives such as surface roughness, MRR, tool life, cutting forces, vibrations, etc. (Fu et al., 2012; Josyula and Narala, 2018; Lu et al., 2009; Nalbant et al., 2007; Sivasakthivel et al., 2017; Tzeng et al., 2009; Winter et al., 2013).

The commonly used optimization techniques are ANN, GA, desirability analysis, RSM, Taguchi approach, etc. The existing review studies in the field of machining parameter optimization have been reviewed and discussed in chapter 2. It is evident from the literature review that R_a is the most widely used optimization objective. But, in

practice, surface finish is generally known *a priori* by the design of the part. In industry, R_a below the desired value is generally acceptable but it is not a need (Pusavec et al., 2015). Improving surface finish beyond a limit leads to an exponential increase in the energy requirement and decreases production rate. Whereas, lowering surface finish beyond a value leads to higher rejects, rework and time (Kant and Sangwan, 2014). Therefore, the surface finish should be targeted for the required value as per the part design requirement and need not to be improved unnecessarily. Energy consumption and MRR are other two important optimization objectives in the literature. The increasing focus of governments, businesses and society has led to carbon emissions (CE) as an objective for the machining industry. These four machining objectives share a complex correlation. For example, power consumption is reduced by lowering the surface finish, surface finish is improved by decreasing the production rate and an increase in production rate leads to increase in power consumption. Therefore, a meaningful optimization must consider these four responses simultaneously. The present study proposes a multi-objective model to minimize the specific energy consumption (SEC) and carbon emissions at five different target surface roughness (R_a) values. A mapping of optimum machining parameters for minimum specific energy consumption and carbon emissions for a range of expected surface finish is provided.

4.2 METHODOLOGY

The research methodology adopted for the present study can be divided into five phases, namely; planning, experimentation and data collection, establishment of predictive models, model testing, and multi-objective optimization. The methodology is shown in Figure 4.1.

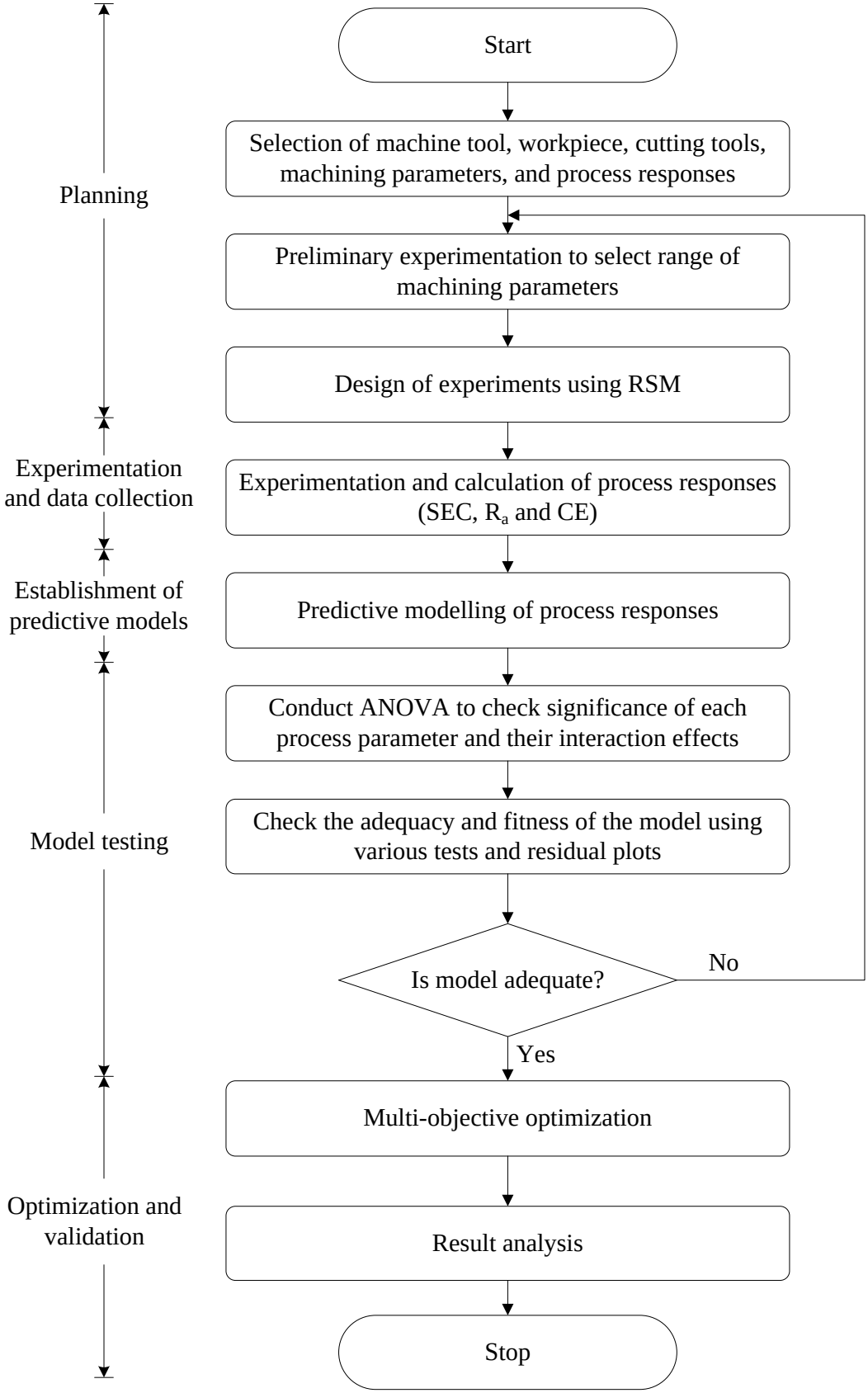

Figure 4.1 Methodology

4.2.1 Planning Phase

4.2.1.1 Selection and modelling of machining parameters

With perusal of relevant literature studies, the important process objectives and parameters were identified which influence the performance and characteristics of the required machining process. The important machining parameters identified were V_c, f, a_p, and a_e. A pilot experimental study was conducted to define the range and levels of these process variables. The details of the machine tool used for experimental investigation, workpiece material, cutting tool, and measurement devices have been provided in chapter 3 (section 3.2). The range of machining parameters was selected considering the machine tool capacity, workpiece and cutting tool material combination, tool manufacturers' recommendations, and the values taken by other researchers in the literature. The range and levels of process parameters selected for the present study are given in Table 4.1. Specific energy consumption, surface roughness and carbon emissions were selected as process responses to study the effect of machining parameters on the machining performance. Two set of experiments were conducted with and without the application of cutting fluid. The mathematical modelling of the process responses is provided as follows:

Table 4.1 Range and levels of machining parameters

Factor	**Representation**	**Level**		
		-1	**0**	**1**
Cutting Speed (RPM)	V_c	1000	2000	3000
Feed (mm/min)	f	200	400	600
Depth of cut (mm)	a_p	0.5	1	1.5
Width of cut (mm)	a_e	4	6	8

i) Specific energy consumption (SEC)

The specific energy consumption of a machining process is defined as the cutting energy used for removing unit volume of workpiece material. In the present study, the total energy consumption of the machine tool from spindle start to spindle stop was considered for calculation of the SEC. The energy required for material removal, spindle rotation and axis movement is influenced by machining parameters; therefore, the total energy consumption including the three energy components is considered for energy modelling here. The power data was recorded at the main electric supply of the machine tool. The power curve was integrated over processing time to calculate the total energy consumption. The power profile of the machining operation is shown in Figure 4.2.

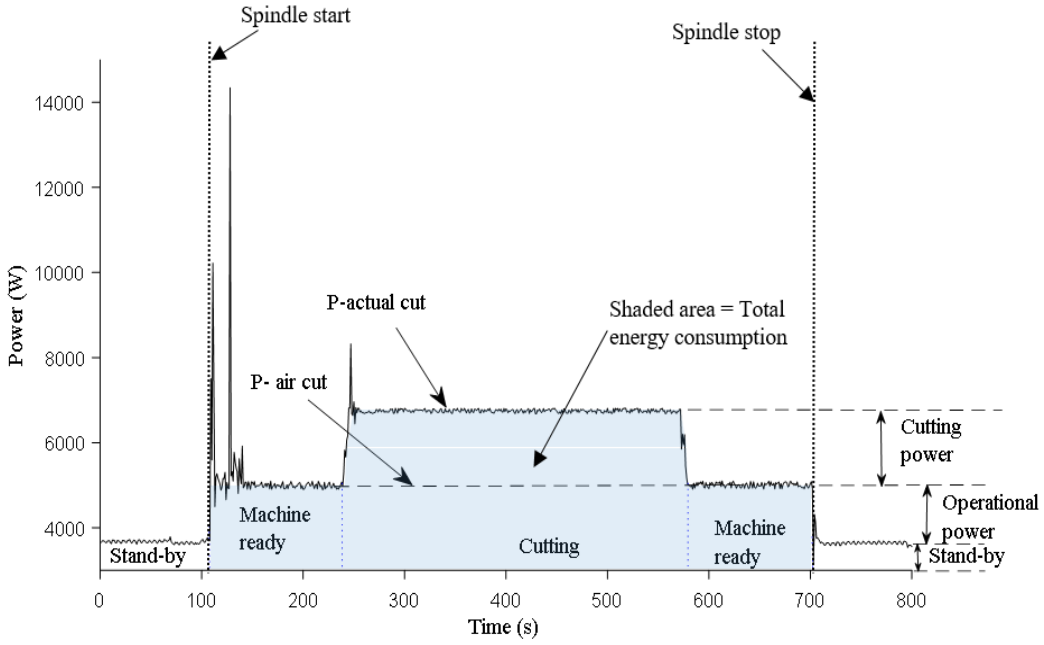

Figure 4.2 Power profile and energy decomposition for the machining process

ii) Surface roughness (R_a)

R_a is a measure of product quality. It was measured at three equi-distant points along the workpiece length and the average was calculated to minimize the probable observation errors.

iii) Carbon emissions (CE)

The mathematical models for the calculation of carbon emissions of the machining process caused by various factors, provided in chapter 3 (section 3.5), are used here. The process parameters have no influence on CE caused by production of raw materials and chip post-processing. As this study aims to analyze the effect of machining parameters on the CE, the CE caused by energy consumption (CE_{energy}), coolant ($CE_{coolant}$) and cutting tools ($CE_{cuttingtool}$) were considered here for calculation of machining carbon emissions. For dry experimental runs, total machining carbon emissions were calculated as a summation of CE_{energy} *and* $CE_{cuttingtool}$. While conducting the experiments with the application of coolant, the tool wear was assumed negligible and therefore total machining carbon emissions were calculated as a summation of CE_{energy} *and* $CE_{coolant}$. The carbon emissions caused due to machining of one cm^3 of material were quantified and used as a process response in the present study.

4.2.1.2 Design of experiments

It is very crucial to derive reliable and explicit conclusions from the experimentation (Bhushan, 2013). The results of any experimental investigation depend on the data collection methodology. In the present study, Taguchi-based experimental design was used for experimental planning. The non-linear behavior of the machining parameters can be analyzed by considering more than two levels of each machining parameter, therefore, in the present study three levels of each machining parameter were selected (Table 4.1). The standard L_{27} orthogonal array is presented in Table 4.2. The columns chosen for main factors are 1, 2, 5, and 6. In the present study, column numbers 1, 2, 5, and 6 were chosen for cutting speed, feed, depth of cut, and width of cut, respectively.

Table 4.2 Standard L_{27} orthogonal array with parameters and interactions

S. No.	Column number												
	1	**2**	**3**	**4**	**5**	**6**	**7**	**8**	**9**	**10**	**11**	**12**	**13**
	A	**B**	**A × B**	**A × B**	**C**	**D**	**E**	**B × C**	**--**	**--**	**B × C**	**--**	**--**
1	-1	-1	-1	-1	-1	-1	-1	-1	-1	-1	-1	-1	-1
2	-1	-1	-1	-1	0	0	0	0	0	0	0	0	0
3	-1	-1	-1	-1	1	1	1	1	1	1	1	1	1
4	-1	0	0	0	-1	-1	-1	0	0	0	1	1	1
5	-1	0	0	0	0	0	0	1	1	1	-1	-1	-1
6	-1	0	0	0	1	1	1	-1	-1	-1	0	0	0
7	-1	1	1	1	-1	-1	-1	1	1	1	0	0	0
8	-1	1	1	1	0	0	0	-1	-1	-1	1	1	1
9	-1	1	1	1	1	1	1	0	0	0	-1	-1	-1
10	0	-1	0	1	-1	0	1	-1	0	1	-1	0	1
11	0	-1	0	1	0	1	-1	0	1	-1	0	1	1
12	0	-1	0	1	1	-1	0	1	-1	0	1	-1	0
13	0	0	1	-1	-1	0	1	0	1	-1	1	-1	0
14	0	0	1	-1	0	1	-1	1	-1	0	-1	0	1
15	0	0	1	-1	1	-1	0	-1	0	1	0	1	-1
16	0	1	-1	0	-1	0	1	1	-1	0	0	1	-1
17	0	1	-1	0	0	1	-1	-1	0	1	1	-1	0
18	0	1	-1	0	1	-1	0	0	1	-1	-1	0	1
19	1	-1	1	0	-1	1	0	-1	1	0	-1	1	0
20	1	-1	1	0	0	-1	1	0	-1	1	0	-1	1
21	1	-1	1	0	1	0	-1	1	0	-1	1	0	-1
22	1	0	-1	1	-1	1	0	0	-1	1	1	0	-1
23	1	0	-1	1	0	-1	1	1	0	-1	-1	1	0
24	1	0	-1	1	1	0	-1	-1	1	0	0	-1	1
25	1	1	0	-1	-1	1	0	1	0	-1	0	-1	1
26	1	1	0	-1	0	-1	1	-1	1	0	1	0	-1
27	1	1	0	-1	1	0	-1	0	-1	1	-1	1	0

4.2.2 Experimentation and Data Collection

After the design of experiments, experiments were performed and required responses were recorded. Two set of experiments were conducted: one under dry (without coolant) and another under wet (with coolant) cutting conditions. The power consumption was recorded at the main supply of the machine tool using NI 9227 and 9244 data acquisition cards and Labview software. The details of the experimental set up and power measuring device are provided in chapter 3 (section 3.2). The surface roughness was measured using Taylor Hobson Talysurf. The carbon emissions were calculated based on the models provided in chapter 3 (section 3.5). The model coefficients used for carbon emissions in the present study are provided in Table 4.3. The experimental results under dry and wet cutting conditions are provided in Table 4.4.

Table 4.3 Calculation parameters used in the present study

Cutting tool coefficients	**C_t**	**m**	**r**	**K**	**N**	**W_{tool}**
	6.41×10^{9}	1.85	1.23	0.63	3	0.14 kg
Calculation parameters	**$T_{coolant}$ (month)**		**V_{in} (m^3)**	**δ**		**V_{ad} (m^3)**
	3		16×10^{-3}	5%		5.5×10^{-3}
	CEF_{energy} ($kgCO_2/kWh$)		**$CEF_{coolant}$ ($kgCO_2/m^3$)**	**$CEF_{coolant-dis}$ ($kgCO_2/m^3$)**		**$CEF_{cutting\ tool}$ ($kgCO_2/kg$)**
	1.41		500	200		31.5

4.2.3 Establishment of Predictive Models for Process Responses

Next, predictive models for the process responses were obtained using response surface methodology (RSM) and the effects of process parameters on the process responses were analyzed. RSM is a collection of statistical and mathematical techniques used for modelling and analysis of the optimization problems where the response is influenced by more than one variables (Kant and Sangwan, 2014). It is a sequential experimental approach for empirical modelling and optimization. It can be used for both first and second order models.

Table 4.4 Experimental results under dry and wet cutting conditions

Experimental run	Cutting speed	Feed	Depth of cut	Width of cut	Dry cutting			Wet cutting		
					SEC (J/mm^3)	R_a (µm)	Carbon emissions (gCO_2/cm^3)	SEC (J/mm^3)	R_a (µm)	Carbon emissions (gCO_2/cm^3)
1	1000	200	0.5	4	174.55	3.311	99.274	485.40	0.655	190.116
2	1000	200	1	6	60.90	3.363	39.797	161.88	0.477	63.404
3	1000	200	1.5	8	29.80	2.539	21.966	80.49	0.527	31.525
4	1000	400	0.5	4	98.50	3.751	74.830	258.60	1.070	101.286
5	1000	400	1	6	33.83	3.745	31.948	86.74	0.936	33.974
6	1000	400	1.5	8	14.81	3.019	19.048	43.93	1.270	17.204
7	1000	600	0.5	4	74.10	4.577	68.816	184.57	1.312	72.292
8	1000	600	1	6	24.39	4.489	30.081	62.28	1.728	24.391
9	1000	600	1.5	8	21.58	4.987	18.571	31.57	2.286	12.364
10	2000	200	0.5	6	141.63	4.117	129.756	343.82	0.631	134.663
11	2000	200	1	8	53.63	2.518	64.115	129.53	0.625	50.734
12	2000	200	1.5	4	72.47	1.778	102.590	174.66	0.769	68.408
13	2000	400	0.5	6	81.65	2.662	119.102	188.00	0.851	73.634
14	2000	400	1	8	30.05	2.305	62.330	70.85	0.873	27.750
15	2000	400	1.5	4	41.48	1.92	103.277	94.17	1.207	36.882
16	2000	600	0.5	6	63.88	4.284	120.659	136.64	1.056	53.516
17	2000	600	1	8	24.86	2.762	65.237	51.85	1.427	20.308
18	2000	600	1.5	4	30.02	2.706	107.297	68.50	1.562	26.829
19	3000	200	0.5	8	122.09	3.282	165.774	274.40	0.599	107.474
20	3000	200	1	4	121.54	1.549	230.147	275.09	0.616	107.743
21	3000	200	1.5	6	56.48	1.316	126.866	121.71	0.723	47.670
22	3000	400	0.5	8	73.69	2.182	167.204	151.41	0.795	59.304
23	3000	400	1	4	73.05	0.825	242.706	150.58	0.751	58.976
24	3000	400	1.5	6	32.48	0.987	135.569	66.90	0.995	26.203
25	3000	600	0.5	8	50.95	2.747	171.821	111.70	0.918	43.749
26	3000	600	1	4	56.69	1.401	257.224	106.46	0.966	41.698
27	3000	600	1.5	6	25.03	1.936	144.658	49.16	1.355	19.255

However, second order model is widely used due to its flexibility, ease to estimate regression coefficients, and practical applications. Central composite design (CCD) is commonly used to fit quadratic response models. CCD results in high accuracy for a smaller number of experiments. A quadratic response surface model obtained using RSM is given by equation (4.1).

$$Y = \beta_0 + \sum_{i=1}^{m} \beta_i X_i + \sum_{i=1}^{m} \beta_{ii} X_i^2 + \sum_{j<i} \sum \beta_{ij} X_i X_j + \varepsilon \quad (4.1)$$

where Y and m represent the response variable and number of variables, respectively. The terms β_0, β_i, β_{ii}, and β_{ij} are regression constants. The terms X_i, X_i^2, $X_i X_j$ are linear, quadratic and interaction terms for cutting parameters and ε is the arbitrary error due to measurement, background noise, etc. The detailed analysis of the experimental results and predictive modelling for the dry and wet cutting experiments are presented in the next sections.

4.2.4 Error Analysis of the Predictive Models

The mathematical models formulated above were tested for accuracy and adequacy using ANOVA, error analysis, normal distribution plot, and residual analysis.

4.2.5 Multi-objective Optimization of the Process Parameters

The machining parameters were optimized for the minimization of specific energy consumption and carbon emissions while maintaining the required surface quality using two multi-objective optimization approaches – desirability approach and multi-objective genetic algorithm (MOGA). The mathematical models of objectives and methodologies used for the data analysis in the present study are explained next.

4.3 PREDICTIVE MODELLING OF PROCESS RESPONSES FOR DRY CUTTING

4.3.1 Predictive Modelling for Specific Energy Consumption

The mathematical model for the prediction of specific energy consumption was obtained using RSM, based on the experimental results presented in Table 4.4. The predictive model for specific energy consumption is as follows:

$$SEC = 488 + 0.012 * \mathrm{V}_c - 0.6463 * \mathrm{f} - 306.8 * \mathrm{a}_p - 35.54 * \mathrm{a}_e + 0.000004 * \mathrm{V}_c * \mathrm{V}_c + 0.000341 * \mathrm{f} * \mathrm{f} + 76 * \mathrm{a}_p * \mathrm{a}_p + 2.544 * \mathrm{a}_e * \mathrm{a}_e - 0.000009 * \mathrm{V}_c * \mathrm{f} + 0.01331 * \mathrm{V}_c * \mathrm{a}_p - 0.00527 * \mathrm{V}_c * \mathrm{a}_e + 0.1393 * \mathrm{f} * \mathrm{a}_p + 0.02075 * \mathrm{f} * \mathrm{a}_e \quad (4.2)$$

The values of SEC for each experimental run were calculated using the predictive model and compared with the experimentally obtained values (Figure 4.3). It is observed that the predicted values of SEC are close to the experimentally measured values. The mean relative error between the experimental and predictive values is 7.31%.

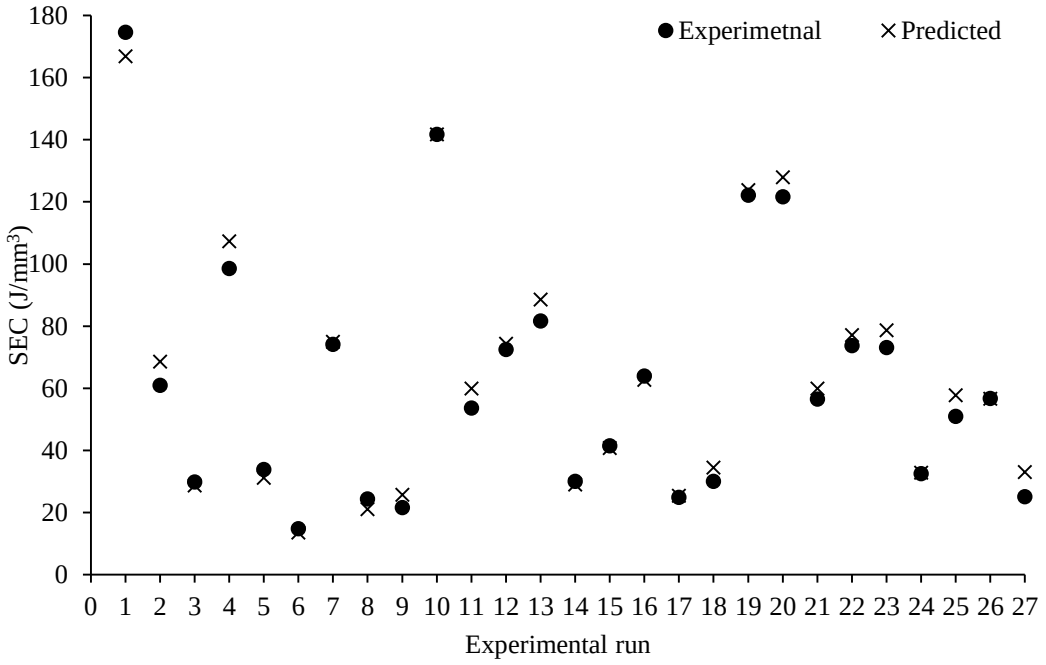

Figure 4.3 Experimentally measured and predicted values of SEC for dry cutting

The mathematical model obtained by using RSM was further analyzed by using analysis of variance (ANOVA). It is used to determine the relative importance of each process parameter and their interaction effect on SEC and the adequacy of the model. ANOVA was performed with 95% confidence level and 5% significance level. Table 4.5 shows the ANOVA results for SEC during dry cutting.

Table 4.5 ANOVA results for SEC during dry cutting

Source	**DF**	**Adj SS**	**Adj MS**	**F-Value**	**P-Value**	**% contribution**	**Remarks**
Model	13	41458.4	3189.1	109.54	0	99.10	
Linear	4	29313.1	7328.3	251.71	0	70.07	$F^{standard}_{(0.05,13,26)}$=2.11
V_c	1	351.5	351.5	12.07	0.004	0.84	
f	1	11837.2	11837.2	406.58	0	28.29	$F^{regression} > F^{standard}_{(0.05,13,26)}$
a_p	1	11798.5	11798.5	405.25	0	28.20	
a_e	1	1892.8	1892.8	65.01	0	4.52	
Square	4	3099.2	774.8	26.61	0	7.41	
$V_c \times V_c$	1	78.6	78.6	2.7	0.124	0.19	
f × f	1	1116.4	1116.4	38.35	0	2.67	
$a_p \times a_p$	1	1626.1	1626.1	55.85	0	3.89	model is adequate
$a_e \times a_e$	1	465.9	465.9	16	0.002	1.11	
2-Way Interaction	5	3709.4	741.9	25.48	0	8.87	
$V_c \times f$	1	41.3	41.3	1.42	0.255	0.10	
$V_c \times a_p$	1	199.3	199.3	6.84	0.021	0.48	
$V_c \times a_e$	1	499.7	499.7	17.16	0.001	1.19	
$f \times a_p$	1	2330	2330	80.03	0	5.57	
$f \times a_e$	1	826.9	826.9	28.4	0	1.98	
Error	13	378.5	29.1			0.90	
Total	26	41836.9				100.00	
R^2 = 99.10%	R^2 (adj.) = 98.19%			R^2 (pred.) = 95.6%			

DF: Degree of freedom, SS: Sum of square, MS: Mean square

The sum of squares in the ANOVA table represents the square of deviation from the mean. Mean squares are obtained by dividing the sum of squares by degrees of freedom. F-value or Fisher value in the ANOVA table is the ratio of the mean square of the model to the mean square of error. It is a measure to predict the importance of the predictive

model with respect to the variance of each term at the desired level of significance. Higher F-value indicates a significant effect of the corresponding parameter. Generally, it is considered that a parameter has significant impact on the response if the F-value is more than four. The F-value is also used to check the adequacy of the model. The calculated F-value of the predictive model was compared with the standard value at the desired significance level. It is apparent from Table 4.5 that the proposed predictive model qualifies the adequacy test as the model F-value (109.54) is higher than the tabulated F-value (2.11) at 95% confidence level.

P-value or probability value indicates the statistical importance of each term for a certain level of confidence. The present analysis has been done at 95% confidence level and 5% significance level, i.e. $\alpha = 0.05$. Therefore, a factor is statistically significant only if its p-value is smaller than 0.05. It is shown in Table 4.5 that all linear terms; square terms of feed, depth of cut and width of cut; interaction terms of cutting speed–depth of cut, cutting speed–width of cut, feed–depth of cut, and feed–width of cut are statistically significant. Feed and depth of cut are the most significant parameters for SEC with percentage contributions of 28.29% and 28.20%, respectively. Further, R^2 is the ratio of explained variation to the total variation in the data. It is used to access model fitness. The value of R^2 is 0.9910 which means that 99.10% of the total variance in the data can be explained by the model. The adjusted R^2 is the value of R^2 for significant terms only after dropping the insignificant terms. Predicted R^2 indicates the value of R^2 for any new data. Here, R^2 (Adj.) is 0.9819 and R^2 (Pred.) is 0.9506, which indicates a very good correlation.

The model adequacy was also analyzed using residuals. Residual is the variation of predicted response from the corresponding observed response. The plot of residual versus predicted response, and normal probability plot were used to analyze the residuals as

shown in Figures 4.4 and 4.5, respectively. For a model to be adequate, the points on the normal probability plot should be in a straight line and the points on the plot of residual versus predicted response should be uniformly distributed. Both the figures indicate that the predictive model is adequate for computing the SEC.

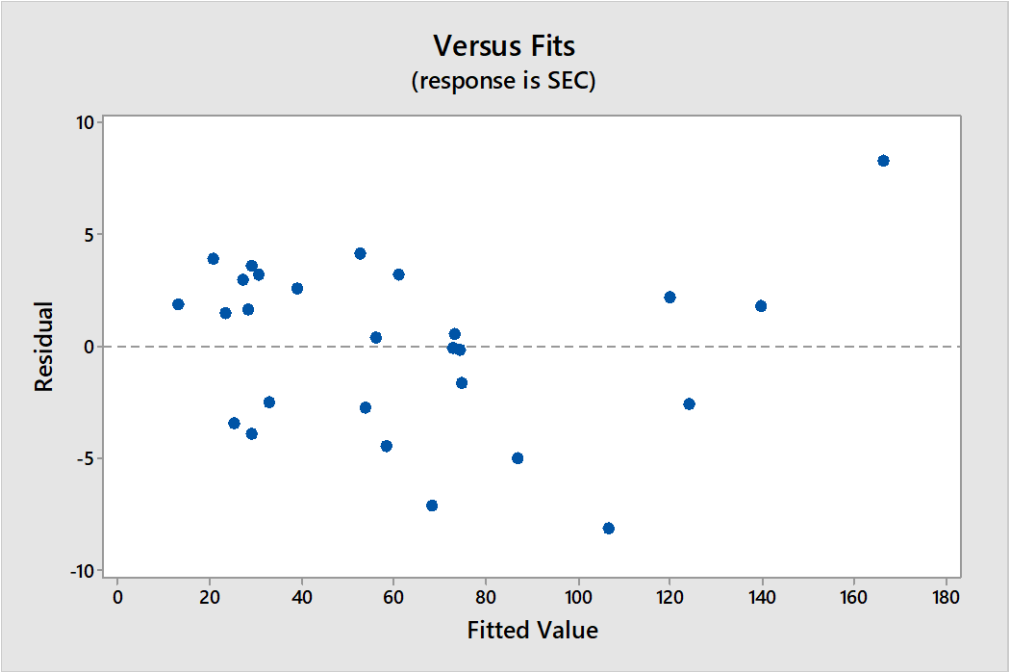

Figure 4.4 Residual v/s fitted value plot for SEC during dry cutting

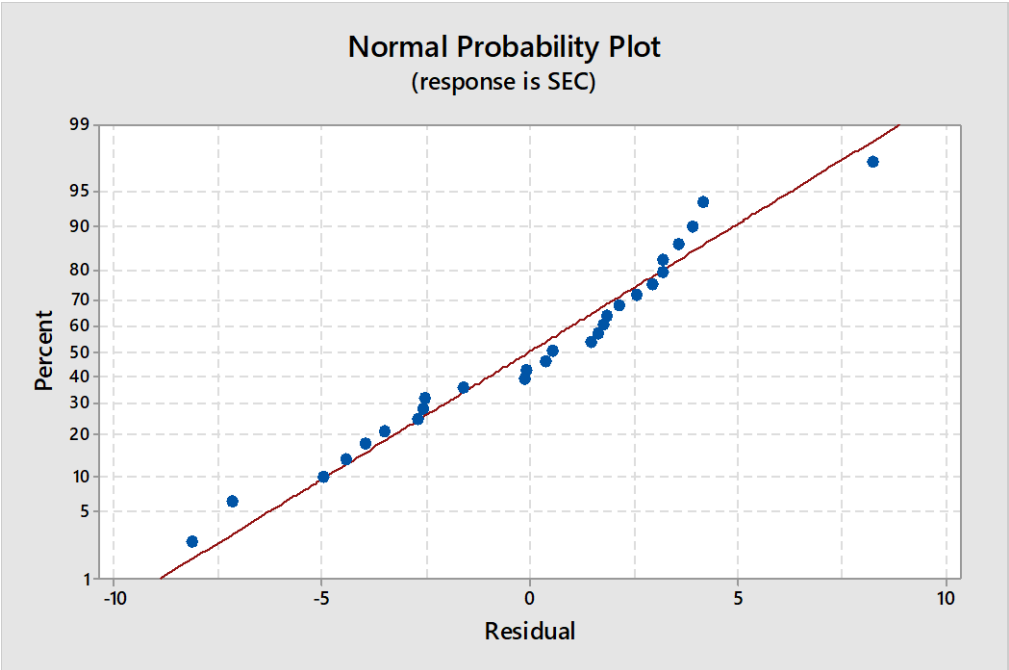

Figure 4.5 Normal probability plot of residuals for SEC during dry cutting

The effect of process parameters on SEC was also studied. Figure 4.6 shows the main effect for SEC during dry experimental runs. It is observed here that the SEC reduces with the increase in feed, depth of cut and width of cut. SEC is the energy required for removing unit volume of workpiece material. Theoretically, SEC is defined as the ratio of power consumption to the material removal rate. With increase in the cutting parameters, MRR increases and leads to reduction in SEC. However, the power consumption for unloaded spindle rotation and movement of feed axes also increase with cutting speed and feed, respectively. After a certain cutting speed is achieved, the increase in power consumption dominates over the increase in MRR, therefore, the SEC increases with increase in cutting speed. The increase in power consumption by axis motors is not significant in the range of feed rate considered in this study. If the feed rate is increased beyond this range, the SEC may increase with increase in feed rate also.

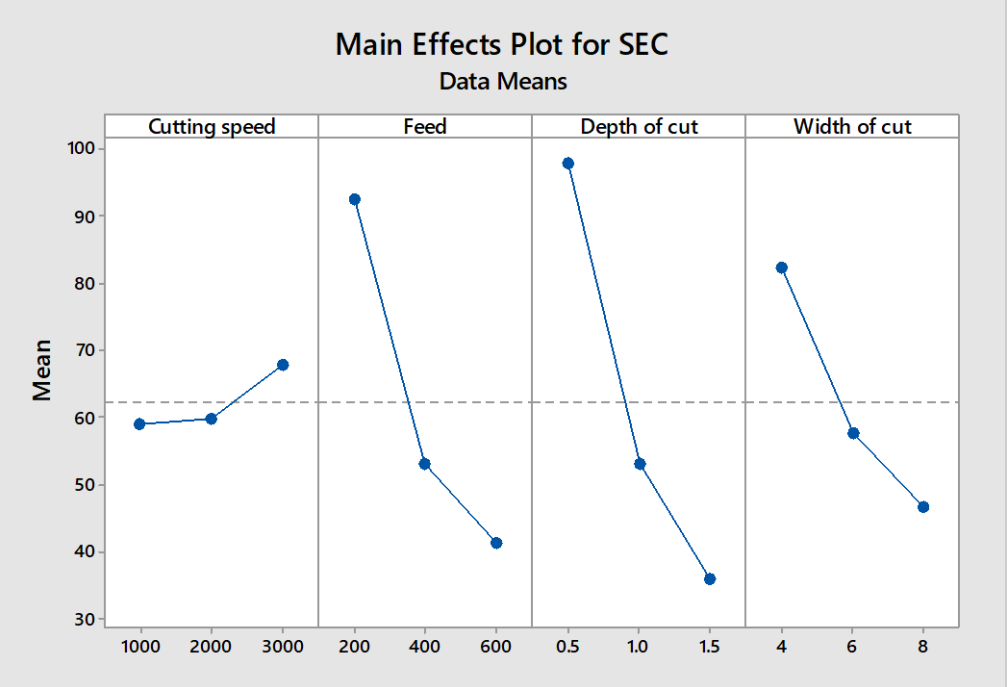

Figure 4.6 Main effect plot for SEC during dry cutting

Figure 4.7 represents the interaction plot for SEC. It is used to analyze the interaction between two parameters. Interaction is significant if the mean response at a parameter level

changes with the level of other parameters. Parallel lines represent the absence of the interaction effect. The degree of interaction increases with increase in deviation of the lines from the parallel state. It is evident from Figure 4.7 that the interaction effect is present between V_c & a_p and V_c & a_e as the lines are intersecting in these cases.

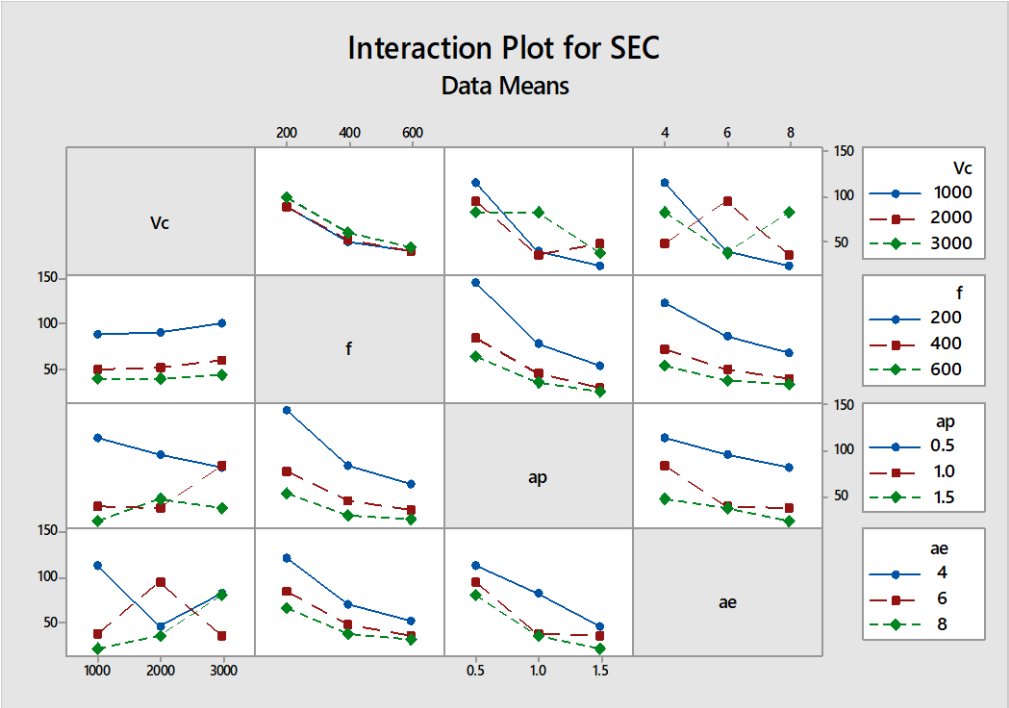

Figure 4.7 Interaction plot for SEC during dry cutting

4.3.2 Predictive Modelling for Surface Roughness

The predictive model for surface roughness was also obtained by using RSM, as follows:

$$R_a = 2.63 + 0.000198 * V_c - 0.009.1 * f - 3.18 * a_p + 1.346 * a_e + 0.000015 * \mathrm{f} * \mathrm{f} + 1.191 * a_p * a_p - 0.1165 * a_e * a_e - 0.000002 * V_c * \mathrm{f} - 0.000611 * V_c * a_p + 0.000046 * V_c * a_e + 0.002582 * \mathrm{f} * a_p + 0.000023 * \mathrm{f} * a_e \quad (4.3)$$

The values of surface roughness for each experimental run were calculated using the predictive model and compared with the experimentally obtained values (Figure 4.8). The

mean relative error between the experimental and predictive values was 6.98%. The mathematical model obtained by using RSM was further analyzed using analysis of variance (ANOVA) with 95% confidence level and 5% significance level. Table 4.6 shows the ANOVA results for surface roughness during dry experimental runs.

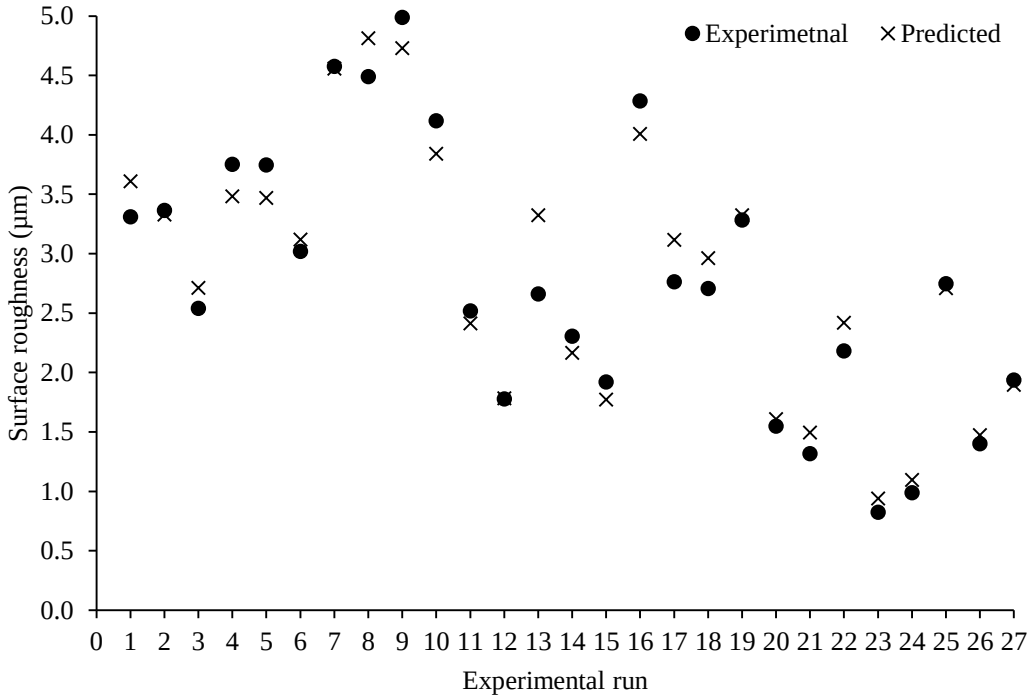

Figure 4.8 Experimentally measured and predicted values of surface roughness during dry cutting

It is apparent here that the proposed predictive model qualifies the adequacy test as the model F-value (24.2) is higher than the tabulated F-value (2.11) at 95% confidence level. The value of R^2 is 0.9603 which means that 96.03% of the total variance in the data can be explained by the model. The values of R^2(adj.) and R^2(pred.) are 0.9206 and 0.8359, respectively. It shows that the model can explain 83.59% variance for new data. The model adequacy has also been analyzed using residuals.

The plot of residual versus predicted response, and normal probability plot are used to analyze the residuals as shown in Figures 4.9 and 4.10, respectively. It is observed that the points on the normal probability plot are close to the straight line and the points on the plot

of residual versus predicted response are uniformly distributed. Both the figures indicate that the predictive model is adequate for the prediction of surface roughness under dry cutting conditions.

Table 4.6 ANOVA results for surface roughness during dry cutting

Source	**DF**	**Adj SS**	**Adj MS**	**F-Value**	**P-Value**	**% contribution**	**Remarks**
Model	13	32.324	2.487	24.2	0	96.03	
Linear	4	21.406	5.351	52.09	0	63.59	
V_c	1	17.123	17.123	166.68	0	50.87	$F^{standard}_{(0.05,13,26)}$=2.11
f	1	2.078	2.078	20.23	0.001	6.17	
a_p	1	2.198	2.198	21.4	0	6.53	$F^{regression} > F^{standard}_{(0.05,13,26)}$
a_e	1	0.087	0.087	0.85	0.373	0.26	
Square	4	3.745	0.936	9.11	0.001	11.12	
$V_c \times V_c$	1	0.000	0.000	0	0.967	0.00	
f × f	1	2.188	2.188	21.3	0	6.50	
$a_p \times a_p$	1	0.399	0.399	3.88	0.071	1.18	model is adequate
$a_e \times a_e$	1	0.977	0.977	9.51	0.009	2.90	
2-Way Interaction	5	3.246	0.649	6.32	0.003	9.64	
$V_c \times f$	1	2.003	2.003	19.5	0.001	5.95	
$V_c \times a_p$	1	0.420	0.420	4.09	0.064	1.25	
$V_c \times a_e$	1	0.038	0.038	0.37	0.553	0.11	
f × a_p	1	0.800	0.800	7.79	0.015	2.38	
f × a_e	1	0.001	0.001	0.01	0.922	0.00	
Error	13	1.336	0.103			3.97	
Total	26	33.660				100.00	
R^2 = 96.03%	R^2 (adj.) = 92.06%			R^2 (pred.) = 83.59%			

DF: Degree of freedom, SS: Sum of square, MS: Mean square

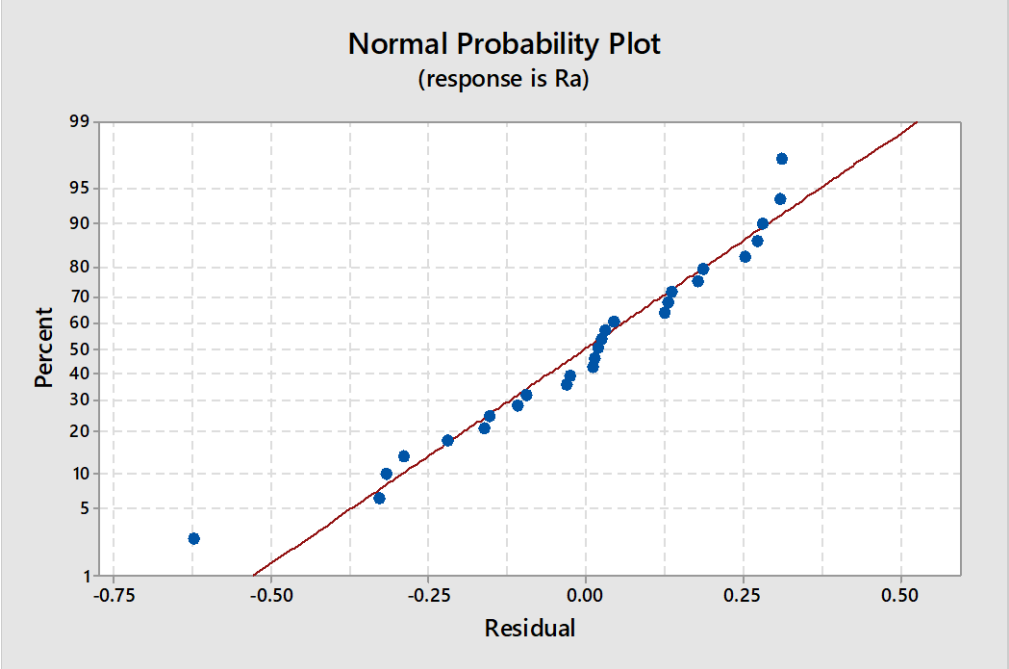

Figure 4.9 Normal probability plot of residuals for SEC during dry cutting

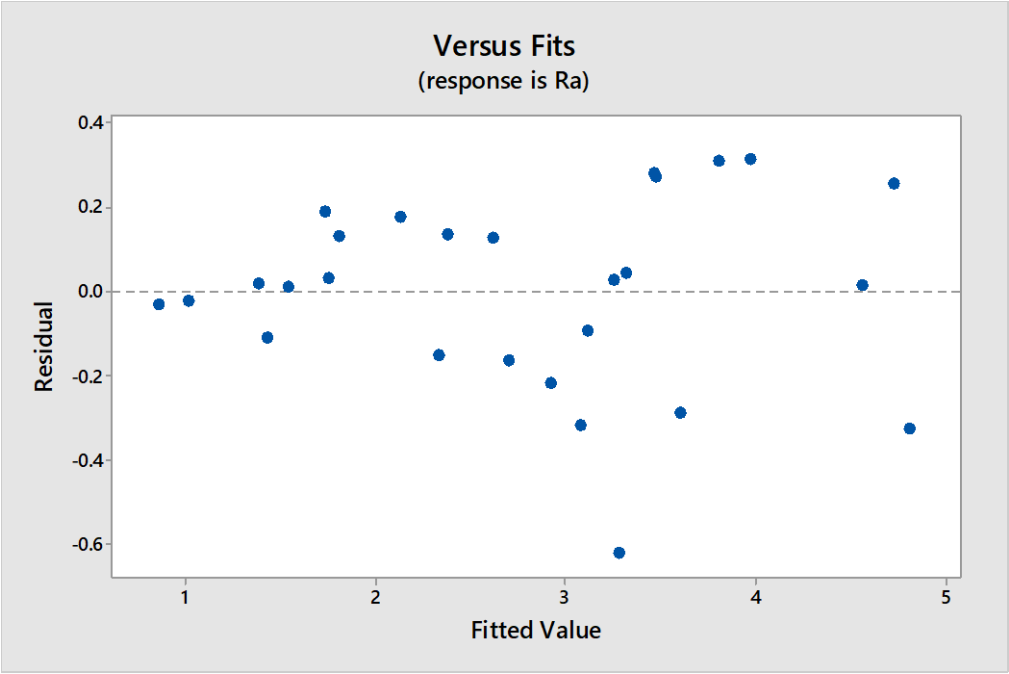

Figure 4.10 Residual v/s fitted value plot for surface roughness during dry cutting

The main effect plot and interaction plot for surface roughness during dry experimental runs show the effect of process parameters and their interaction on surface roughness (Figures 4.11 and 4.12).

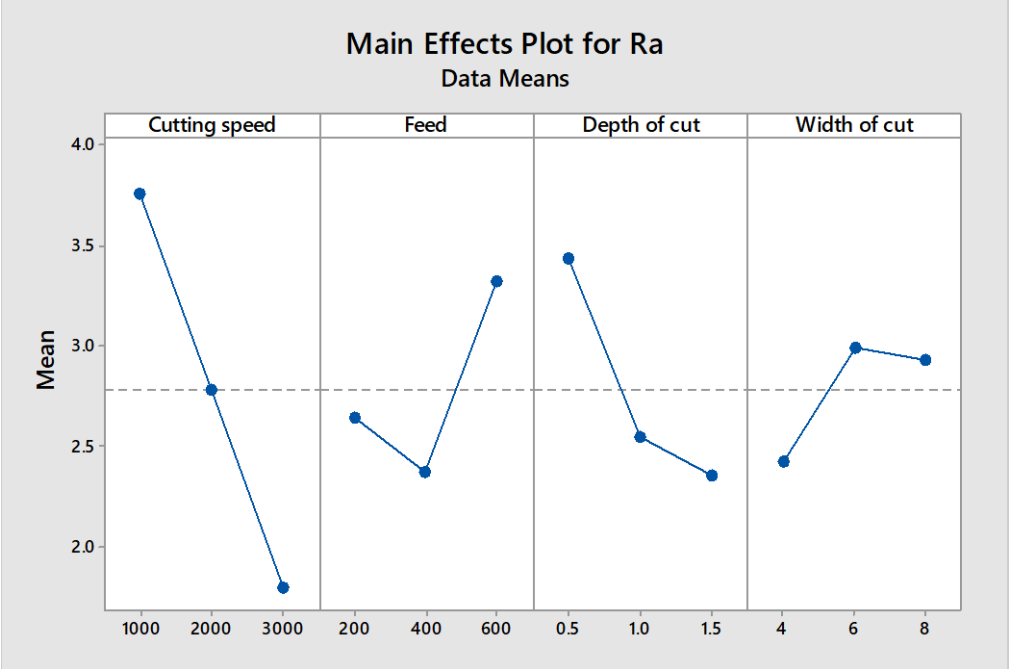

Figure 4.11 Main effect plot for surface roughness during dry cutting

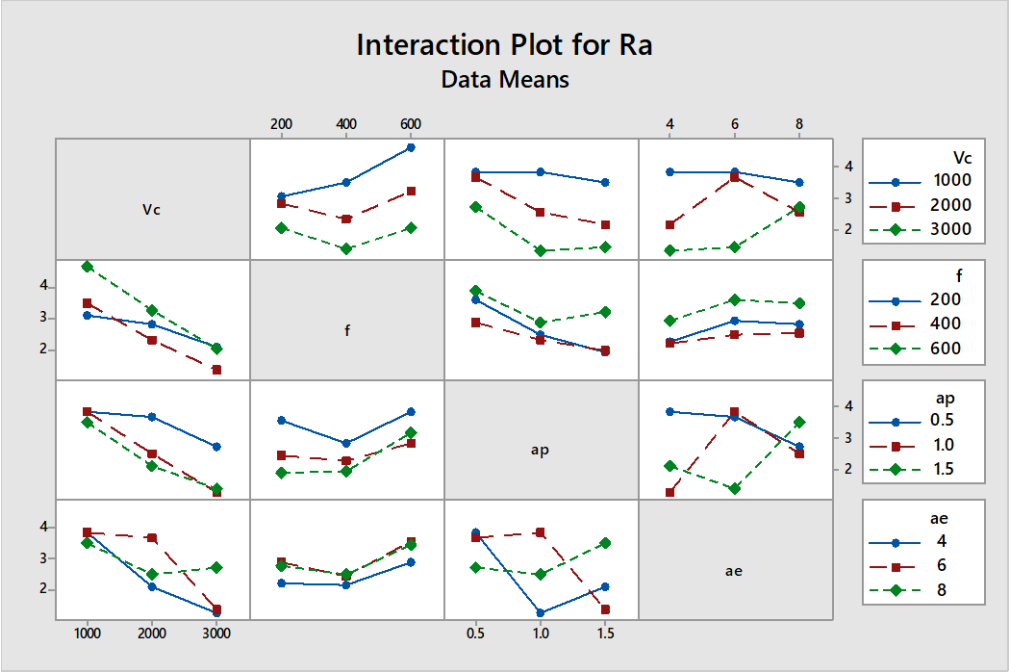

Figure 4.12 Interaction plot for surface roughness during dry cutting

The surface finish improved with increase in cutting speed. This is supported by the statement that cutting forces reduce at higher cutting speeds leading to lower vibration and better surface finish. Also, the tendency of built-up edge (BUE) formation reduces at higher cutting speeds which leads to better surface finish. This explains that higher cutting

speed is favorable for better surface roughness. At lower feed rates, the feed had little influence on surface roughness; but at higher feed, the surface roughness increased with increase in feed. It was also observed that the surface roughness reduced with higher depth of cut. With increase in width of cut, it first increased and then starts to decrease.

4.3.3 Predictive Modelling for Carbon Emissions

The predictive model for carbon emissions obtained using RSM, is as follows:

$$CE = 169.0 + 0.08403 * V_c - 0.1830 * f - 86.6 * a_p - 25.04 * a_e + 0.000017 * V_c * V_c + 0.000073 * f * f + 19.84 * a_p * a_p + 2.879 * a_e * a_e + 0.000039 * V_c * f - 0.01735 * V_c * a_p - 0.013299 * V_c * a_e + 0.0438 * f * a_p + 0.00051 * f * a_e \quad (4.4)$$

The values of carbon emissions for each experimental run were calculated using the predictive model and compared with the experimentally obtained values (Figure 4.13). It was observed that the predicted values of carbon emissions were close to the experimentally measured values. The mean relative error between the experimental and predictive values was 3.16 %.

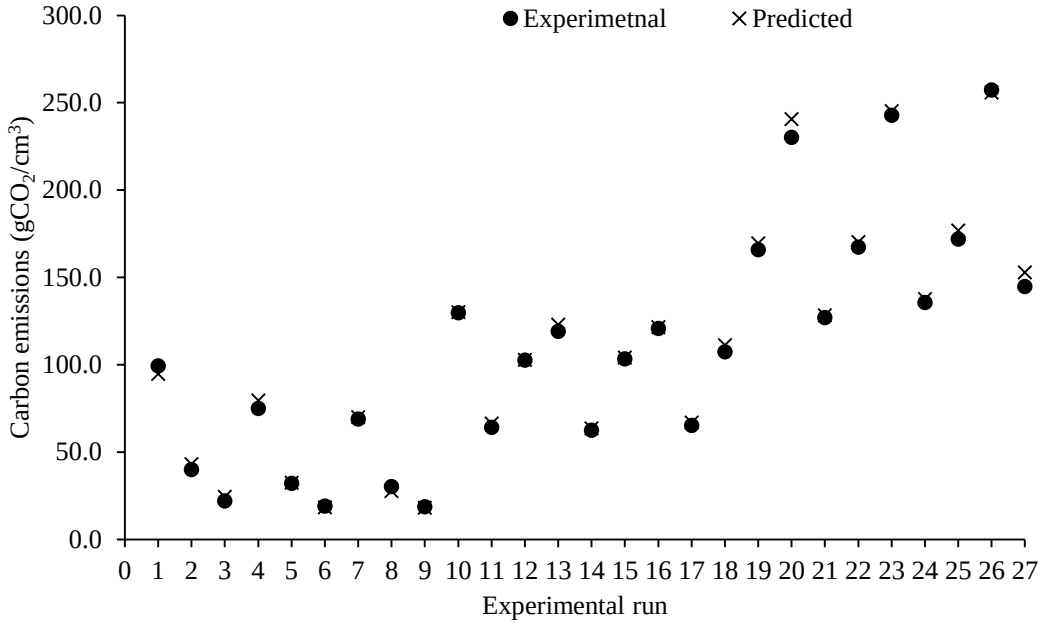

Figure 4.13 Experimentally measured and predicted values of CE during dry cutting

The relative importance of each process parameter, their interaction effect on CE and the adequacy of the model was tested using ANOVA with 95% confidence level and 5% significance level. Table 4.7 shows the ANOVA results for CE during dry experimental runs. The tabulated F-value of the model at 95% confidence level is 2.11. The model F-value (646.67) is higher than the standard tabulated value, which indicates the adequacy of the prediction model. It was also observed that the cutting speed had highest impact on carbon emissions with a percentage contribution of 72.18%.

Table 4.7 ANOVA results for carbon emissions during dry cutting

Source	**DF**	**Adj SS**	**Adj MS**	**F-Value**	**P-Value**	**% contribution**	**Remarks**
Model	13	117706	9054	646.67	0	99.84	
Linear	4	111112	27778	1983.95	0	94.25	
V_c	1	85097	85097	6077.77	0	72.18	$F^{standard}_{(0.05,13,26)}$=2.11
f	1	1	0.9	0.07	0.801	0.00	
a_p	1	9241	9241	660.01	0	7.84	$F^{regression} > F^{standard}_{(0.05,13,26)}$
a_e	1	10275	10274	733.85	0	8.72	
Square	4	2344	586	41.86	0	1.99	
$V_c \times V_c$	1	1640	1639	117.12	0	1.39	
f × f	1	51	51	3.66	0.078	0.04	
$a_p \times a_p$	1	111	110	7.91	0.015	0.09	model is adequate
$a_e \times a_e$	1	597	596	42.61	0	0.51	
2-Way Interaction	5	7057	1411	100.8	0	5.99	
$V_c \times f$	1	744	743	53.13	0	0.63	
$V_c \times a_p$	1	339	338	24.2	0	0.29	
$V_c \times a_e$	1	3184	3183	227.39	0	2.70	
f × a_p	1	231	230	16.48	0.001	0.20	
f × a_e	1	0	0.5	0.04	0.853	0.00	
Error	13	182	14			0.15	
Total	26	117889				100.00	
R^2 = 99.85%	R^2 (adj.) = 99.69%			R^2 (pred.) = 99.16%			

DF: Degree of freedom, SS: Sum of square, MS: Mean square

The value of R^2 was 0.9985 indicating that 99.85% of the total variance in the data can be explained by the model. R^2 (Adj.) was 0.9969 and R^2 (Pred.) was 0.9916, which indicated a very good correlation. The residual plots were also analyzed to check the model adequacy (Figures 4.14 and 4.15). Both the figures indicate that the predictive model is adequate for the prediction of carbon emissions under dry cutting conditions.

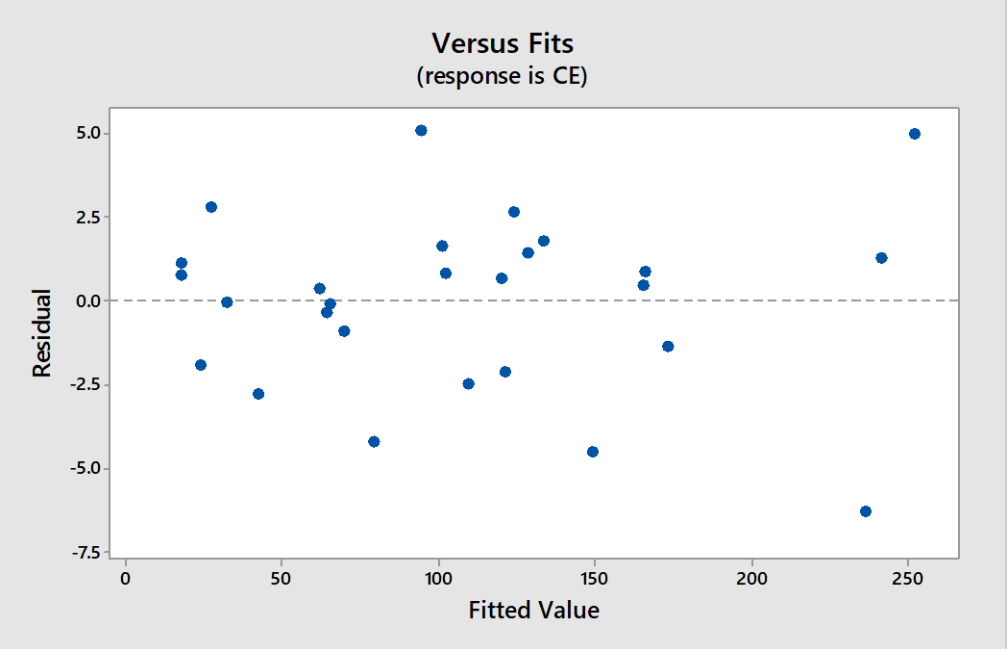

Figure 4.14 Residual v/s fitted value plot for CE during dry cutting

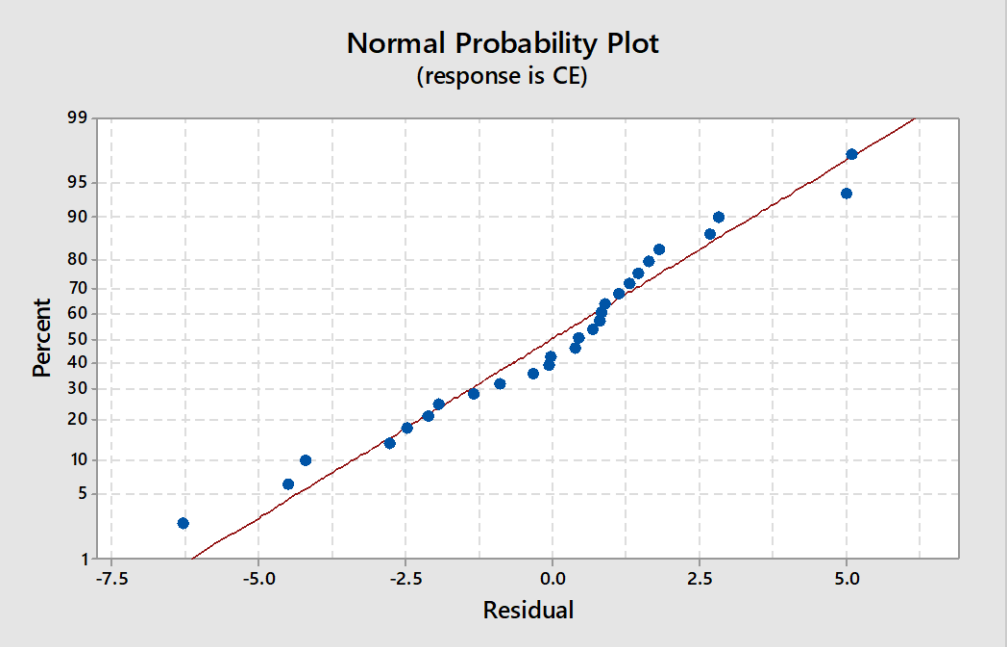

Figure 4.15 Normal probability plot of residuals for CE during dry cutting

The main effect plot and interaction plot for CE under dry experimental conditions are shown in Figure 4.16 and 4.17, respectively. The carbon emissions due to energy consumption and tool wear were considered here, as explained in section 4.2.1.

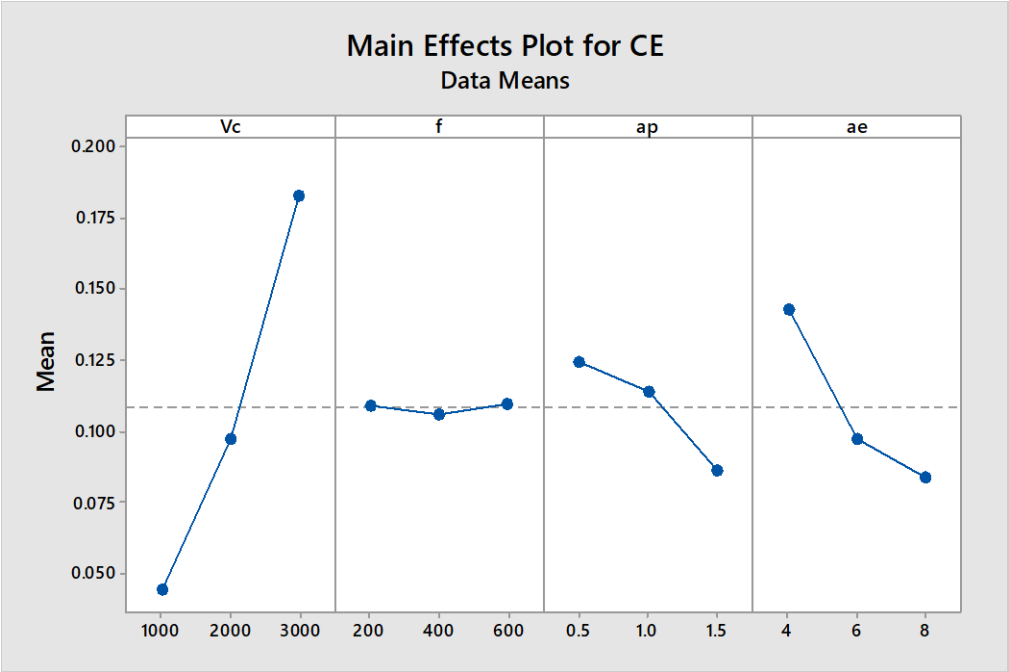

Figure 4.16 Main effect plot for CE during dry cutting

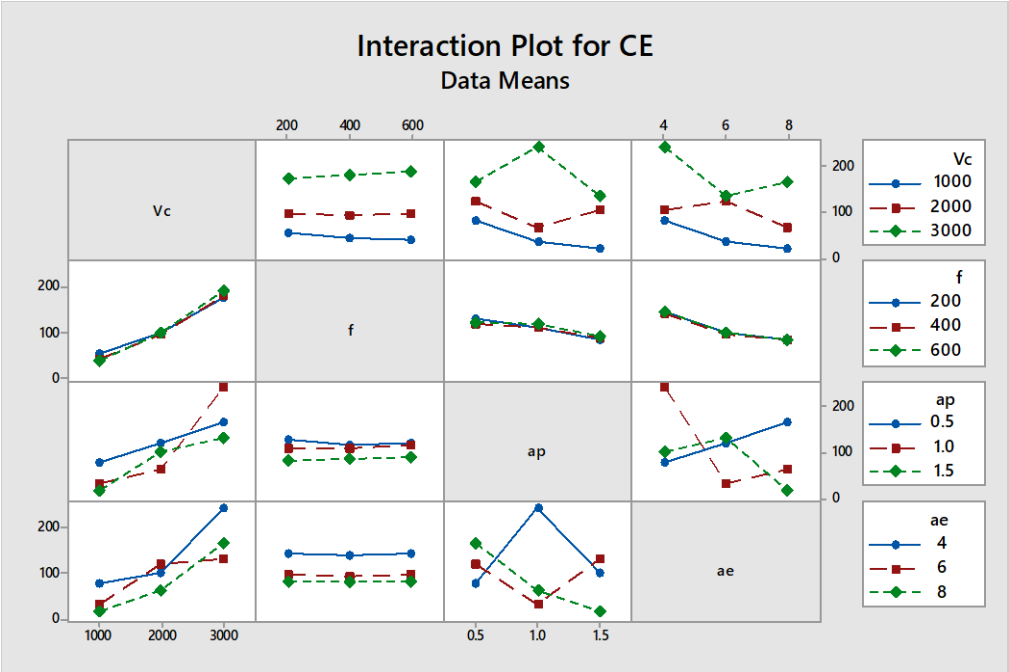

Figure 4.17 Interaction plot for CE during dry cutting

It was observed from Figure 4.16 that the CE increased with increase in cutting speed. The increase in CE was due to the increase in the energy consumption with increase in cutting speed. The variation in CE with change in feed was very small. The CE reduced with depth of cut and width of cut. This may be due to higher MRR at higher depth of cut and width of cut, which lead to lower processing time and lower carbon emissions for machining one cm^3 of workpiece material. The interaction plot shows that the variation of CE with feed is insignificant at any values of cutting speed, depth of cut and width of cut.

4.4 MULTI-OBJECTIVE OPTIMIZATION OF PROCESS PARAMETERS

In this section, a multi-objective optimization was performed to minimize the specific energy consumption and carbon emissions while targeting the surface roughness for pre-defined values. In the present study, the surface roughness was given five different target values and the optimization was conducted for five cases as follows:

Case 1: Minimize R_a, SEC and CE

Case 2: Target $R_a = 1\mu m$ and minimize SEC & CE

Case 3: Target $R_a = 2\mu m$ and minimize SEC & CE

Case 4: Target $R_a = 3\mu m$ and minimize SEC & CE

Case 5: Target $R_a = 4\mu m$ and minimize SEC & CE

The study was conducted for each case to analyze the variation in SEC and CE with different targets values of R_a by using two methodologies: desirability analysis and genetic algorithms.

4.4.1 Multi-objective Optimization using Desirability Approach

The cutting parameters were optimized using desirability approach. The desirability function for each response was calculated based upon the characteristics of response variables using following equations.

If the response is to be maximized,

$$d(y_i) = \begin{pmatrix} 0 & if\ y_i \le A_i \\ \left(\frac{y_i - A_i}{C_i - A_i}\right)^s & if\ A_i \le y_i \le C_i \\ 1 & if\ y_i \ge C_i \end{pmatrix} \quad (4.5)$$

If the response is to be minimized,

$$d(y_i) = \begin{pmatrix} 1 & if\ y_i \le A_i \\ \left(\frac{C_i - y_i}{C_i - A_i}\right)^t & if\ A_i \le y_i \le C_i \\ 0 & if\ y_i \ge C_i \end{pmatrix} \quad (4.6)$$

If the response is given a target,

$$d(y_i) = \begin{pmatrix} 0 & if\ y_i \le A_i \\ \left(\frac{y_i - A_i}{B_i - A_i}\right)^s & if\ A_i \le y_i \le B_i \\ 1 & if\ y_i = B_i \\ \left(\frac{y_i - C_i}{B_i - C_i}\right)^t & if\ B_i \le y_i \le C_i \\ 0 & if\ y_i \ge C_i \end{pmatrix} \quad (4.7)$$

where A, B and C are the lowest acceptable, target, and highest permissible values for each response, respectively. Here, s and t are the weights assigned to the response variables ranging from 0.1 to 10. It indicates the shape function of the desirability. If the weight assigned to a response is less than one, it indicates that less emphasis has been put on the target. If the weight is equal to one, it indicates equal importance for target and the bounds. In the current study, both *s* and *t* are chosen to be unity. Hence, the shape function is linear as shown in Figure 4.18. The calculation of individual desirability of each response for the second experimental run is provided below:

$d(SEC) = \left(\frac{174.55-60.9}{174.55-13.58}\right)^1 = 0.7060;$ $\quad d(CE) = \left(\frac{257.22-39.79}{257.22-18.57}\right)^1 = 0.9111$

If surface roughness is to be minimized; $\quad d(R_a) = \left(\frac{4.987-3.363}{4.987-0.825}\right)^1 = 0.3902$

If target surface roughness = 1 µm; $d(R_a) = \left(\frac{3.363-4.987}{1-4.987}\right)^1 = 0.4073$

If target surface roughness = 2 µm; $d(R_a) = \left(\frac{3.363-4.987}{2-4.987}\right)^1 = 0.5437$

If target surface roughness = 3 µm; $d(R_a) = \left(\frac{3.363-4.987}{3-4.987}\right)^1 = 0.8173$

If target surface roughness = 4 µm; $d(R_a) = \left(\frac{3.363-0.825}{4-0.825}\right)^1 = 0.7993$

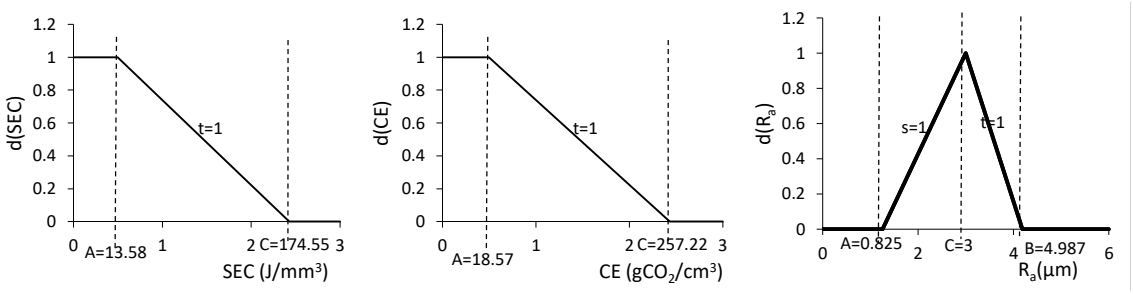

Figure 4.18 Shape functions for desirability of responses

Further, individual desirability (d) is a measure of optimization of a single response and composite desirability (D) is a measure of joint optimization of a set of responses. Composite desirability is the weighted geometric mean of the discrete desirability for each response.

$$D = ({d_1}^{u_1} \times {d_2}^{u_2} \times \ldots \times {d_n}^{u_n})^{\frac{1}{\sum u_i}} = (\prod_{i=1}^{n} {d_i}^{u_i})^{\frac{1}{\sum u_i}} \quad (4.8)$$

where u_i is the importance factor for each response variable ranging between 0.1 and 10. The responses, which are more important for the study, are assigned higher importance factor. In the present study, each response had significant impact on the output and held equal importance. So the default value of unity was assigned for each response. The calculation of composite desirability for the first experimental run is shown as follows:

If surface roughness is to be minimized; $D = (0.706 * 0.9111 * 0.3902)^{\frac{1}{3}} = 0.6313$

If target surface roughness = 1 μm; $D = (0.706 * 0.9111 * 0.4073)^{\frac{1}{3}} = 0.6403$

If target surface roughness = 2 μm; $D = (0.706 * 0.9111 * 0.5437)^{\frac{1}{3}} = 0.7051$

If target surface roughness = 3 μm; $D = (0.706 * 0.9111 * 0.8173)^{\frac{1}{3}} = 0.8077$

If target surface roughness = 4 μm; $D = (0.706 * 0.9111 * 0.7993)^{\frac{1}{3}} = 0.8017$

Once individual desirability for each process response was calculated, the weighted geometric mean was calculated to signify the overall desirability of the multiple objective function. The optimization problem was thus reduced to single objective problem. Thereafter, composite desirability was maximized using reduced gradient algorithm. This algorithm starts with multiple possible solutions and converges to the final optimal solution (Maji et al., 2013). Constraints for process variable values; starting points for the search algorithm and properties of the confidence intervals were defined. With all this information, the response optimizer software computed an optimal solution and presented the variation of each response with process parameters with a desirability plot. The sensitivity analysis can be performed by changing the input variable settings in this interactive plot and the initial solution can be improved. The response optimizer software also facilitates the modification of the variable settings interactively. In the present study, the entire calculation was repeated five times for different target surface roughness values and the optimization plots are shown in Figures 4.19 – 4.23.

Multi-objective optimization plot for the target surface roughness value of 1μm is shown in Figure 4.20. Here, the composite desirability is 0.7163 and individual desirability for R_a, CE and SEC are 0.9484, 0.5347, and 0.7248, respectively. As individual desirability for R_a is highest, it can be quoted that the present setting of input parameters is most effective for achievement of target surface roughness value followed by minimization of

SEC and CE, respectively. Similarly, the other optimization plots were analyzed. The optimization results for each case are presented in Table 4.8.

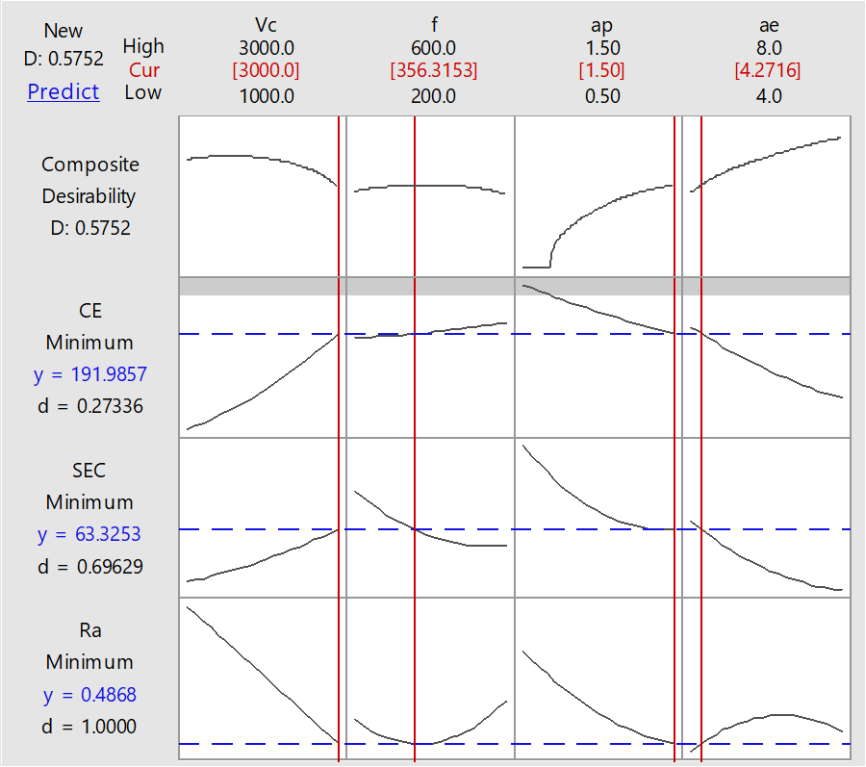

Figure 4.19 Optimization plot for case 1 (Minimization of R_a) during dry cutting

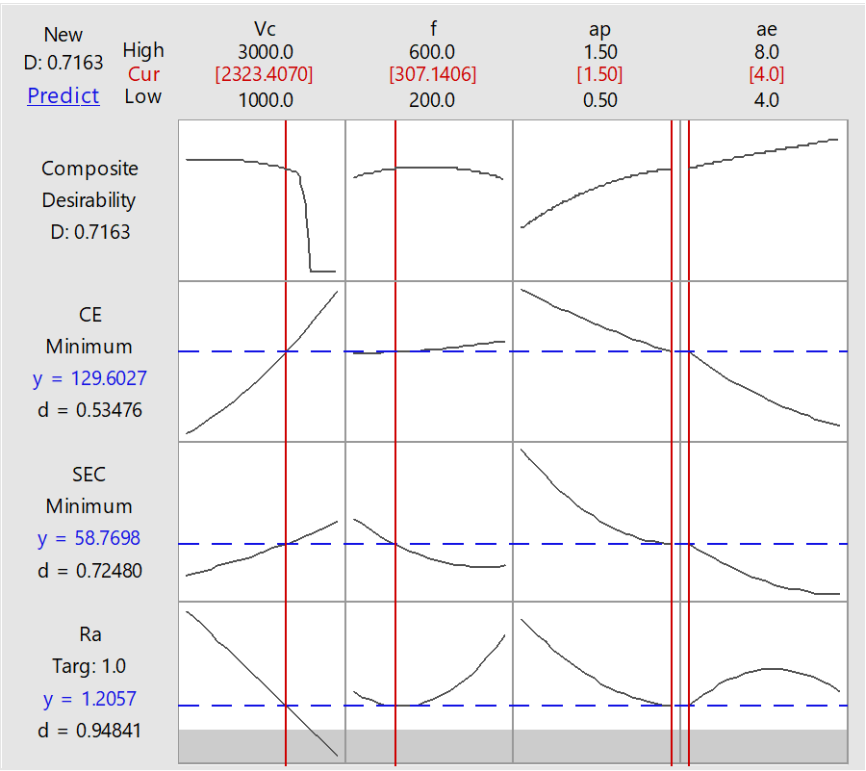

Figure 4.20 Optimization plot for case 2 (Target R_a = 1 µm) during dry cutting

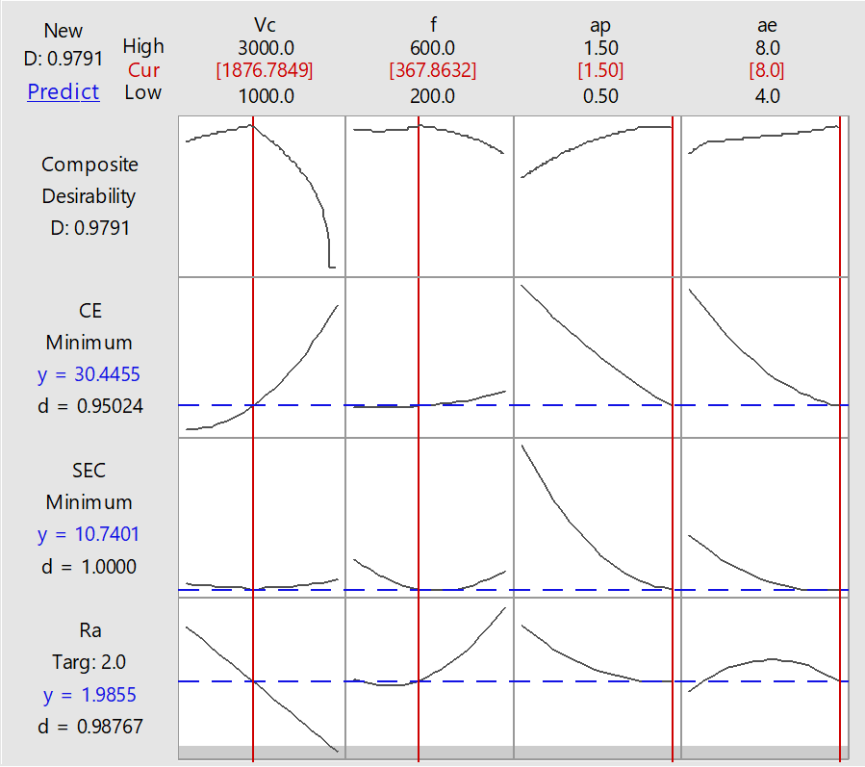

Figure 4.21 Optimization plot for case 3 (Target R_a = 2 µm) during dry cutting

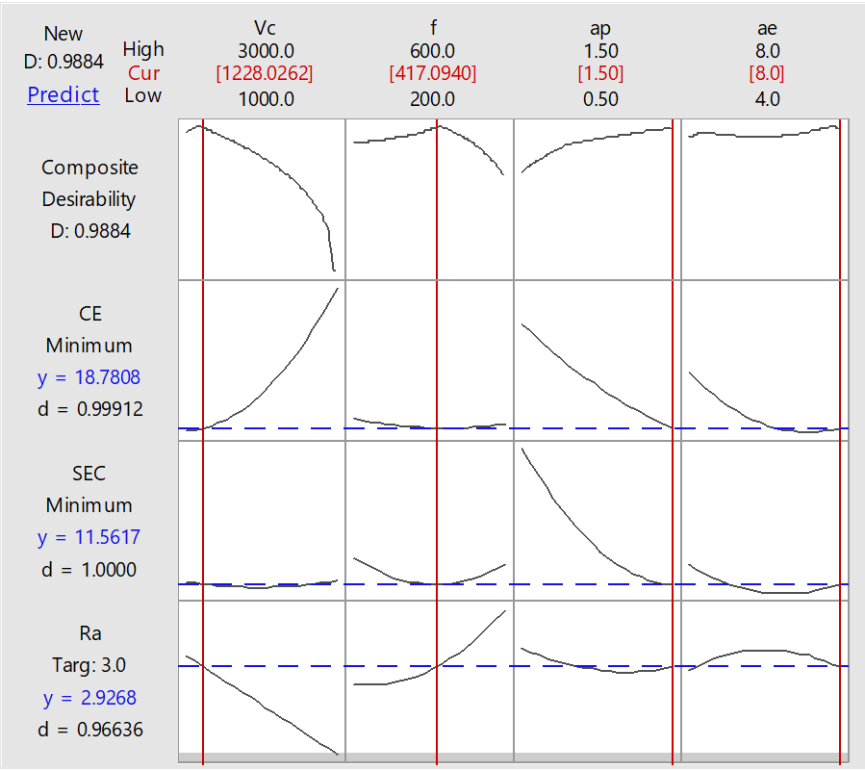

Figure 4.22 Optimization plot for case 4 (Target R_a = 3 µm) during dry cutting

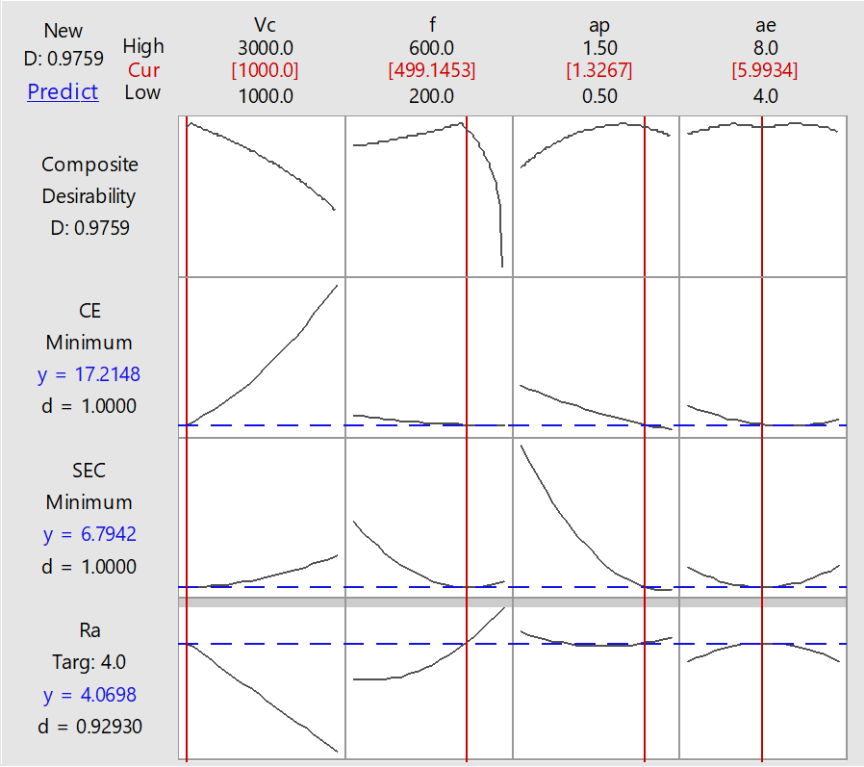

Figure 4.23 Optimization plot for case 5 (Target R_a = 4 µm) during dry cutting

Table 4.8 Multi-objective optimization results (dry cutting) using desirability approach

	V_c (RPM)	f (mm/rev)	a_p (mm)	a_e (mm)	R_a (µm)	SEC (J/mm^3)	CE (gCO_2/cm^3)
Case 1 (Minimization of R_a)	3000	356	1.5	4.27	0.486	63.32	191.98
Case 2 (Target R_a = 1)	2323	307	1.5	4	1.205	58.76	129.60
Case 3 (Target R_a = 2)	1876	367	1.5	8	1.985	10.74	30.44
Case 4 (Target R_a = 3)	1228	417	1.5	8	2.926	11.56	18.78
Case 5 (Target R_a = 4)	1000	499	1.32	5.99	4.060	6.79	17.21

4.4.2 Multi-objective Optimization using MOGA

In the present study, multi-objective optimization was also performed using multi-objective genetic algorithm in MATLAB15 software. The initial parameters were selected as: Population size=50, crossover fraction=0.8, pareto front population factor=0.35, and number of iterations=600. First, multi-objective optimization was performed without any constraint for surface roughness and then constraint functions were used to keep the

surface roughness value less than 1µm, 2µm, 3µm, and 4µm, respectively. The pareto charts for the four cases with different constraint functions for surface roughness are given in Figure 4.24. The optimization results are given in Table 4.9.

Table 4.9 Multi-objective optimization results (dry cutting) using MOGA

	V_c (RPM)	f (mm/rev)	a_p (mm)	a_e (mm)	R_a (µm)	SEC (J/mm^3)	CE (gCO_2/cm^3)
Case 1 (Minimization of R_a)	2976	340	1.5	4	0.466	74.81	203.16
Case 2 (Target R_a = 1)	2818	388	1.5	4.7	0.996	49.50	160.68
Case 3 (Target R_a = 2)	2395	384	1.5	8	1.483	13.61	52.62
Case 4 (Target R_a = 3)	1280	381	1.5	7.2	3.000	9.13	18.57
Case 5 (Target R_a = 4)	1106	475	1.5	6.6	3.856	6.35	14.63

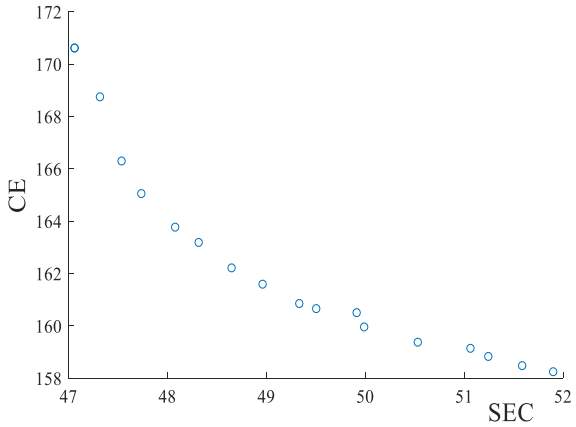

(a) Pareto chart (Target R_a = 1 µm)

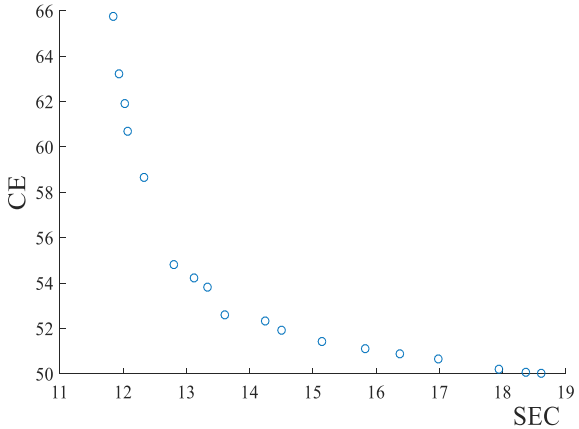

(b) Pareto chart (Target R_a = 2 µm)

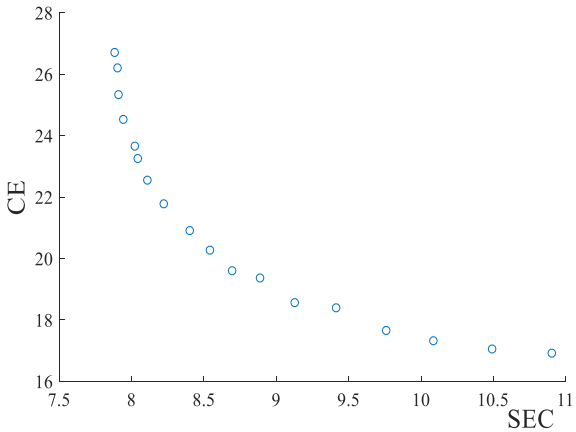

(c) Pareto chart (Target R_a = 3 µm)

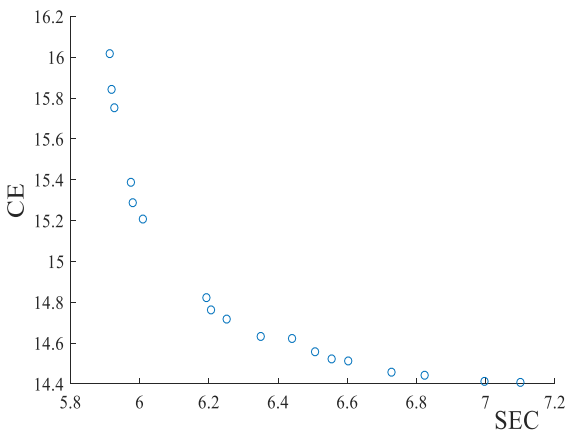

(d) Pareto chart (Target R_a = 4 µm)

Figure 4.24 Pareto charts for multi-objective optimization osing MOGA during dry cutting

4.5 PREDICTIVE MODELLING OF PROCESS RESPONSES DURING WET CUTTING

4.5.1 Predictive Modelling for Specific Energy Consumption

The mathematical model for prediction of specific energy consumption was obtained using RSM, based on the experimental results presented in Table 4.4. The predictive model for specific energy consumption is as follows:

$$SEC = 1427 - 0.0488 * V_c - 1.808 * f - 802.1 * a_p - 112.5 * a_e + 0.000010 * V_c * V_c + 0.000871 * f * f + 188 * a_p * a_p + 7.53 * a_e * a_e + 0.000019 * V_c * f + 0.0517 * V_c * a_p - 0.00949 * V_c * a_e + 0.3692 * f * a_p + 0.0596 * f * a_e \quad (4.9)$$

The values of SEC for each experimental run were calculated using the predictive model and compared with the experimentally obtained values (Figure 4.25). It was observed that the predicted values of SEC were close to the experimentally measured values.

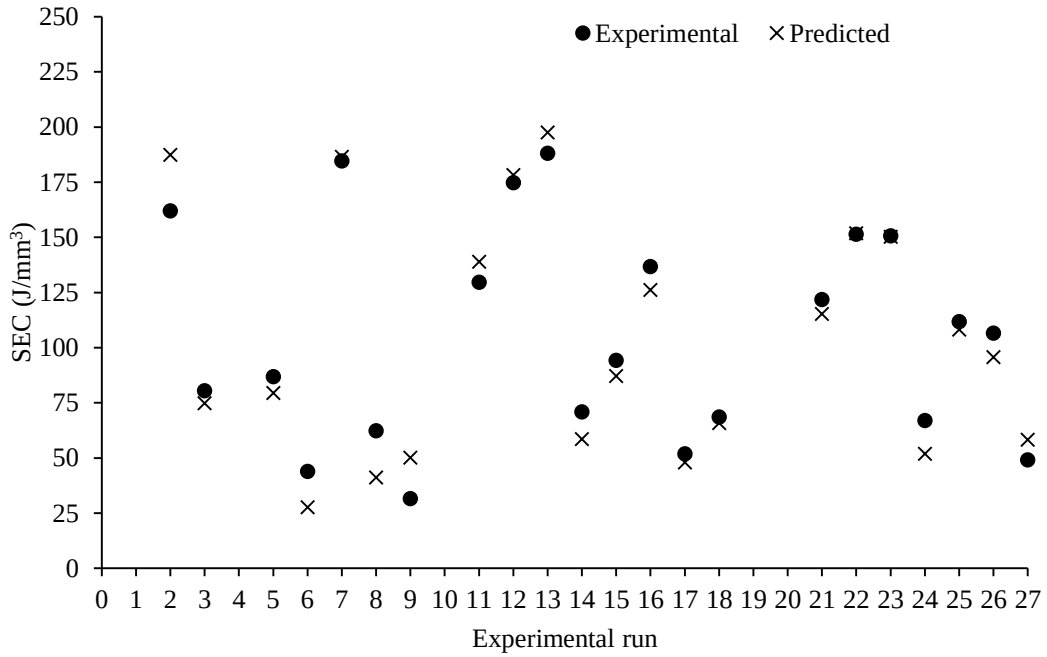

Figure 4.25 Experimentally measured and predicted values of SEC during wet cutting

The mean relative error between the experimental and predictive values was 11.19%. The mathematical model obtained by RSM was further analyzed using analysis of variance (ANOVA). Table 4.10 shows the ANOVA results for SEC during experimental runs during wet cutting.

Table 4.10 ANOVA results for SEC during wet cutting

Source	DF	Adj SS	Adj MS	F-Value	P-Value	% contribution	Remarks
Model	13	280967	21612.8	63.81	0	98.46	
Linear	4	185690	46422.4	137.05	0	65.07	$F^{standard}_{(0.05,13,26)}$=2.11
V_c	1	431	430.6	1.27	0.28	0.15	
f	1	86009	86008.7	253.92	0	30.14	$F^{regression} > F^{standard}_{(0.05,13.26)}$
a_p	1	68844	68843.7	203.25	0	24.12	
a_e	1	10659	10659.1	31.47	0	3.74	
Square	4	20563	5140.7	15.18	0	7.21	
$V_c \times V_c$	1	647	646.5	1.91	0.19	0.23	
f × f	1	7288	7288.3	21.52	0	2.55	
$a_p \times a_p$	1	9939	9938.7	29.34	0	3.48	model is adequate
$a_e \times a_e$	1	4085	4085.1	12.06	0.004	1.43	
2-Way Interaction	5	26594	5318.9	15.7	0	9.32	
$V_c \times f$	1	172	172.4	0.51	0.488	0.06	
$V_c \times a_p$	1	3012	3011.9	8.89	0.011	1.06	
$V_c \times a_e$	1	1621	1621.1	4.79	0.048	0.57	
f × a_p	1	16360	16360	48.3	0	5.73	
f × a_e	1	6831	6830.9	20.17	0.001	2.39	
Error	13	4403	338.7			1.54	
Total	26	285370				100.00	
R^2 = 98.46%	R^2 (adj.) = 96.91%			R^2 (pred.) = 92.14%			

DF: Degree of freedom, SS: Sum of square, MS: Mean square

The plot of residual versus predicted response, and normal probability plot were used to analyze the residuals as shown in Figures 4.26 and 4.27, respectively. Both the figures indicate that the predictive model is adequate for computing the SEC. The effect of process

parameters on SEC was also studied. Figure 4.28 shows the main effect for SEC with application of coolant. It is observed here that the variation in SEC with cutting parameters follow a similar trend with dry experimental runs. Figure 4.29 represents the interaction plot for SEC.

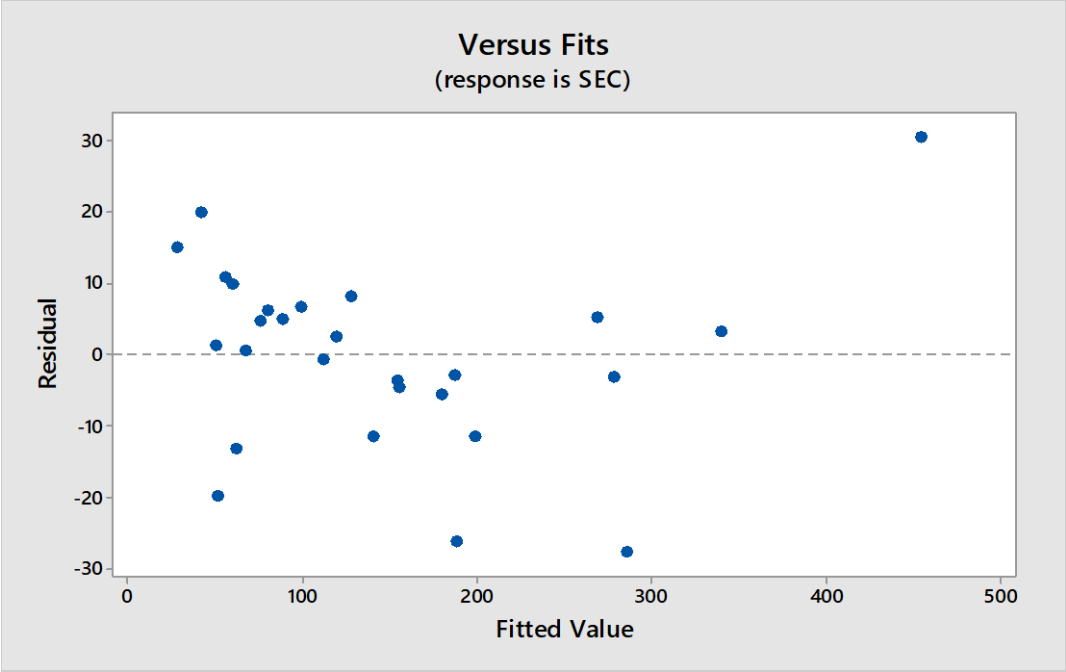

Figure 4.26 Residual v/s fitted value plot for SEC during wet cutting

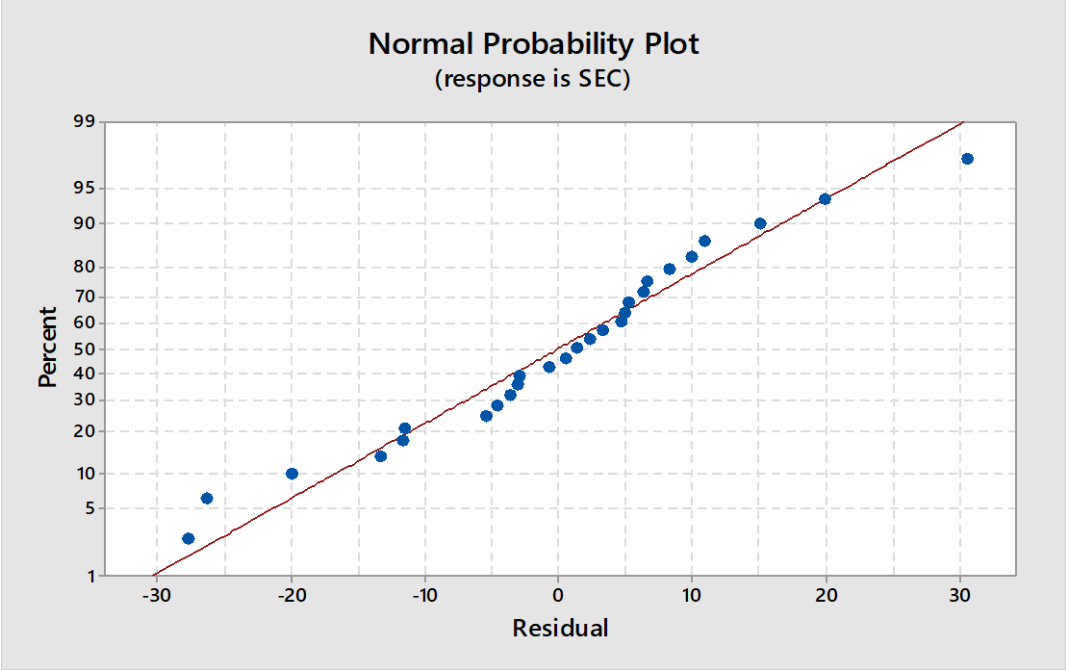

Figure 4.27 Normal probability plot of residuals for SEC during wet cutting

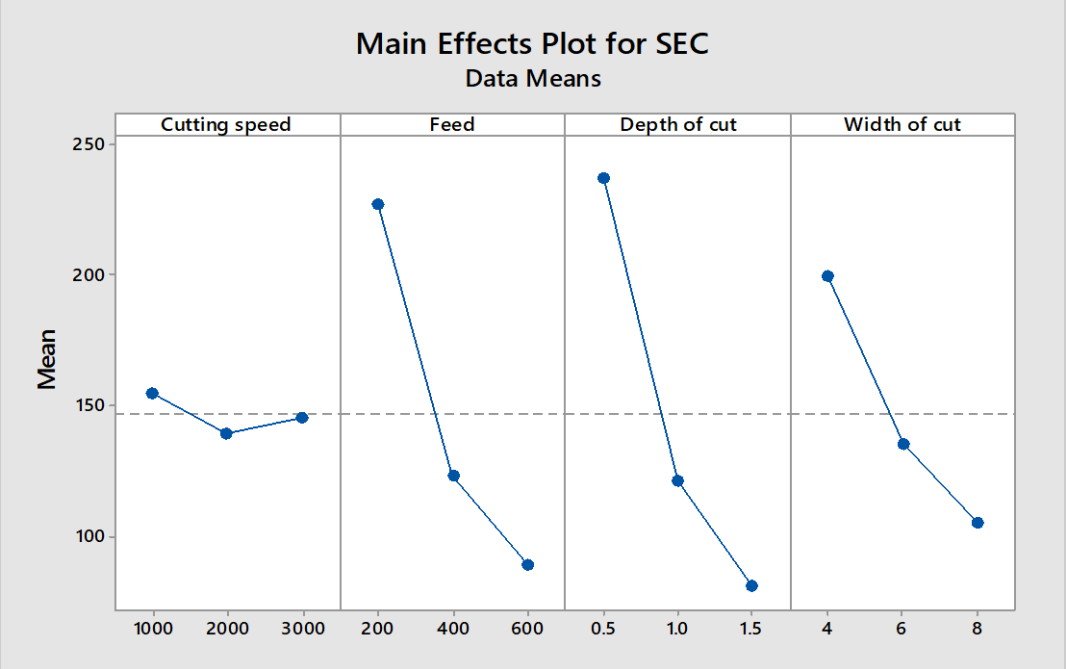

Figure 4.28 Main effect plot for SEC during wet cutting

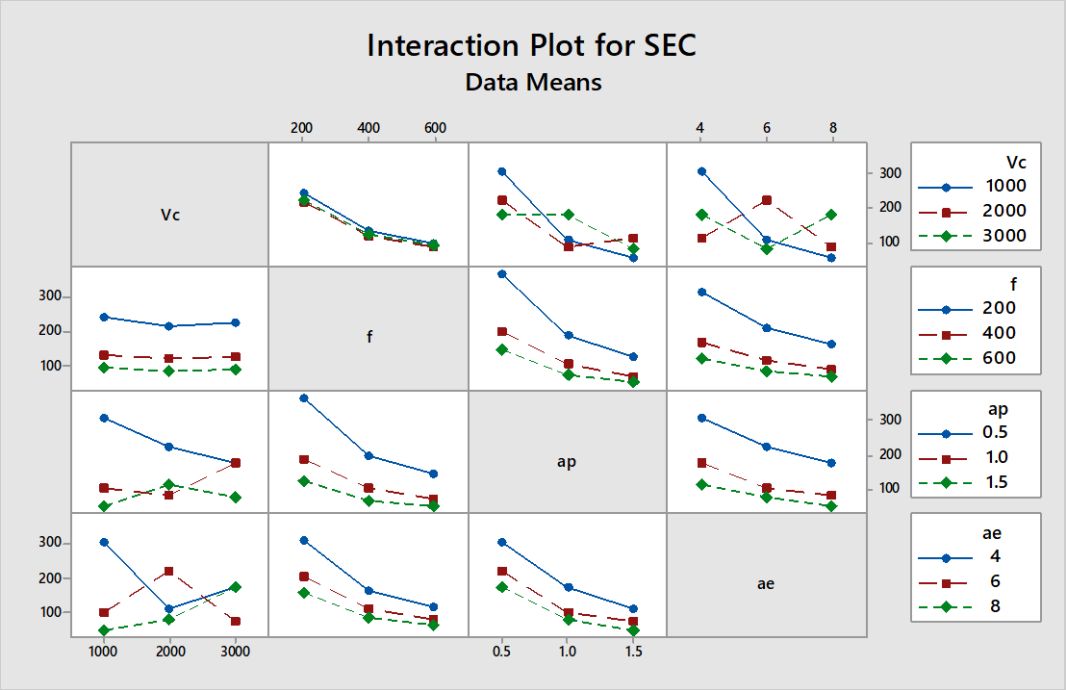

Figure 4.29 Interaction plot for SEC during wet cutting

4.5.2 Predictive Modelling for Surface Roughness

The predictive model for surface roughness was also obtained using RSM, as follows:

$$R_a = 1.314 + 0.000236 * V_c + 0.000259 * f - 1.074 * a_p - 0.209 * a_e + 0.000001 * f * f + 0.388 * a_p * a_p + 0.01067 * a_e * a_e - 0.000001 * V_c * f + 0.000010 * V_c * a_p + 0.000002 * V_c * a_e + 0.001486 * f * a_p + 0.000225 * f * a_e \quad (4.10)$$

The values of surface roughness for each experimental run were calculated using the predictive model and compared with the experimentally obtained values (Figure 4.30). The mean relative error between the experimental and predictive values was 5.11%.

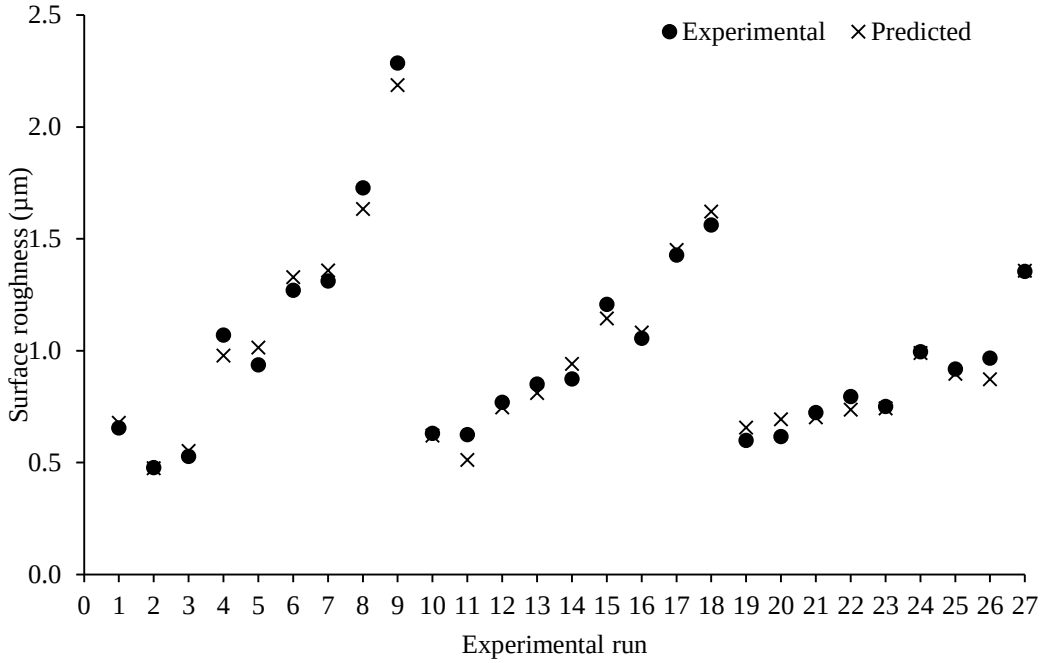

Figure 4.30 Experimentally measured and predicted values of surface roughness during wet cutting

The mathematical model obtained by RSM was further analyzed using analysis of variance (ANOVA) with 95% confidence level and 5% significance level. Table 4.11 shows the ANOVA results for surface roughness during wet experimental runs.

The plot of residual versus predicted response, and normal probability plot were used to analyze the residuals as shown in Figures 4.31 and 4.32, respectively. It is observed that the points on the normal probability plot are close to the straight line and the points on the plot of residual versus predicted response are uniformly distributed. Both the figures

indicate that the predictive model is adequate for the prediction of surface roughness under dry cutting conditions.

Table 4.11 ANOVA results for surface roughness during wet cutting

Source	DF	Adj SS	Adj MS	F-Value	P-Value	% contribution	Remarks
Model	13	4.4269	0.341	50.350	0	98.05	
Linear	4	3.3372	0.834	123.35	0	73.92	
V_c	1	0.3593	0.359	53.120	0	7.96	$F^{standard}_{(0.05,13,26)}$=2.11
f	1	2.7129	2.713	401.10	0	60.09	$F^{regression} > F^{standard}_{(0.05,13,26)}$
a_p	1	0.2247	0.225	33.220	0	4.98	
a_e	1	0.0058	0.006	0.850	0.372	0.13	
Square	4	0.0567	0.014	2.090	0.14	1.25	
$V_c \times V_c$	1	0.0000	0.000	0.000	0.97	0.00	
f × f	1	0.0100	0.010	1.480	0.245	0.22	
$a_p \times a_p$	1	0.0423	0.042	6.260	0.026	0.94	model is adequate
$a_e \times a_e$	1	0.0082	0.008	1.210	0.291	0.18	
2-Way Interaction	5	0.8290	0.166	24.510	0	18.36	
$V_c \times f$	1	0.4665	0.467	68.970	0	10.33	
$V_c \times a_p$	1	0.0001	0.000	0.020	0.902	0.00	
$V_c \times a_e$	1	0.0001	0.000	0.010	0.917	0.00	
$f \times a_p$	1	0.2649	0.265	39.170	0	5.87	
$f \times a_e$	1	0.0972	0.097	14.370	0.002	2.15	
Error	13	0.0879	0.007			1.95	
Total	26	4.5149				100.00	
R^2 = 98.05%	R^2 (adj.) = 96.11%			R^2 (pred.) = 90.91%			

DF: Degree of freedom, SS: Sum of square, MS: Mean square

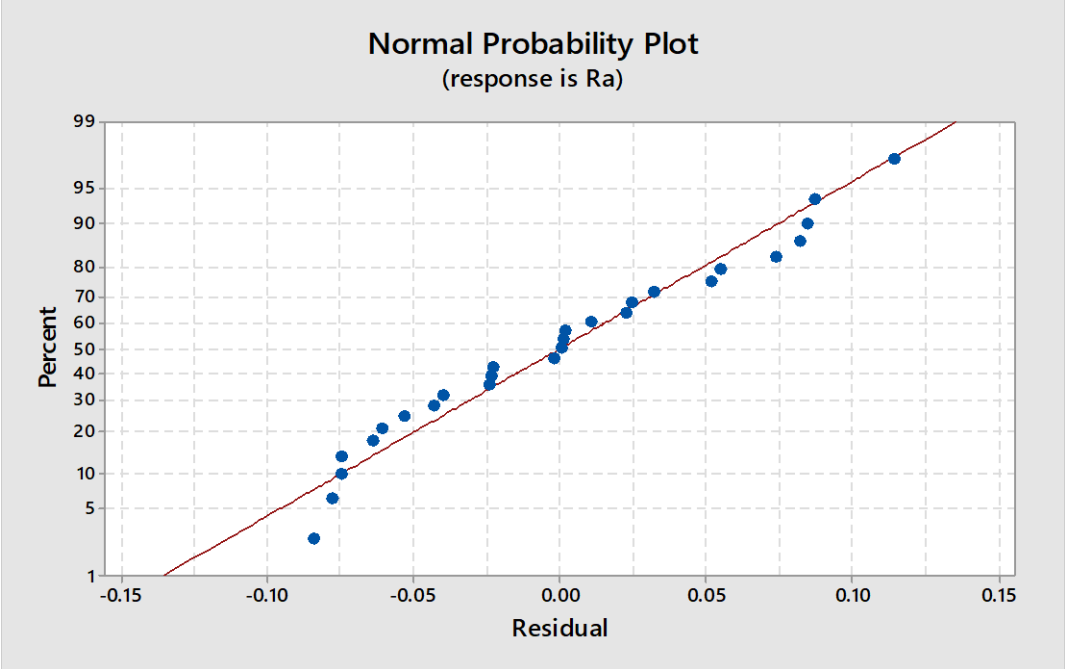

Figure 4.31 Normal probability plot of residuals for surface roughness during wet cutting

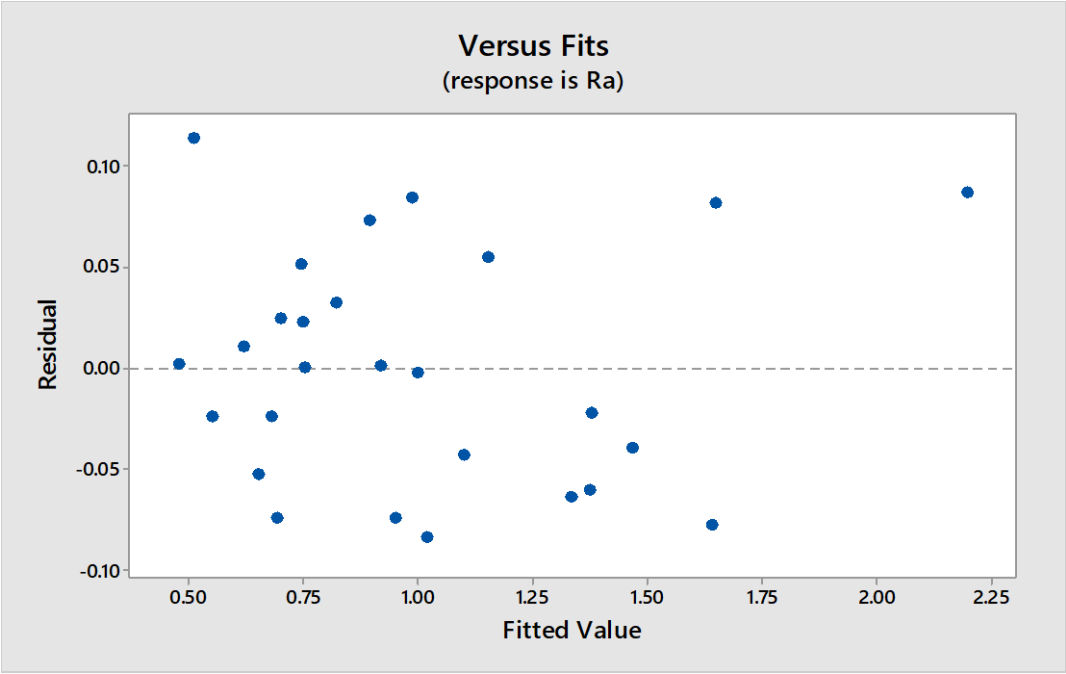

Figure 4.32 Residual v/s fitted value plot for surface roughness during wet cutting

The main effect plot and interaction plot for surface roughness during dry experimental runs show the effect of process parameters and their interaction on surface roughness

(Figures 4.33 and 4.34). The surface roughness reduced with a rise in cutting speed. The width of cut had little influence on surface roughness.

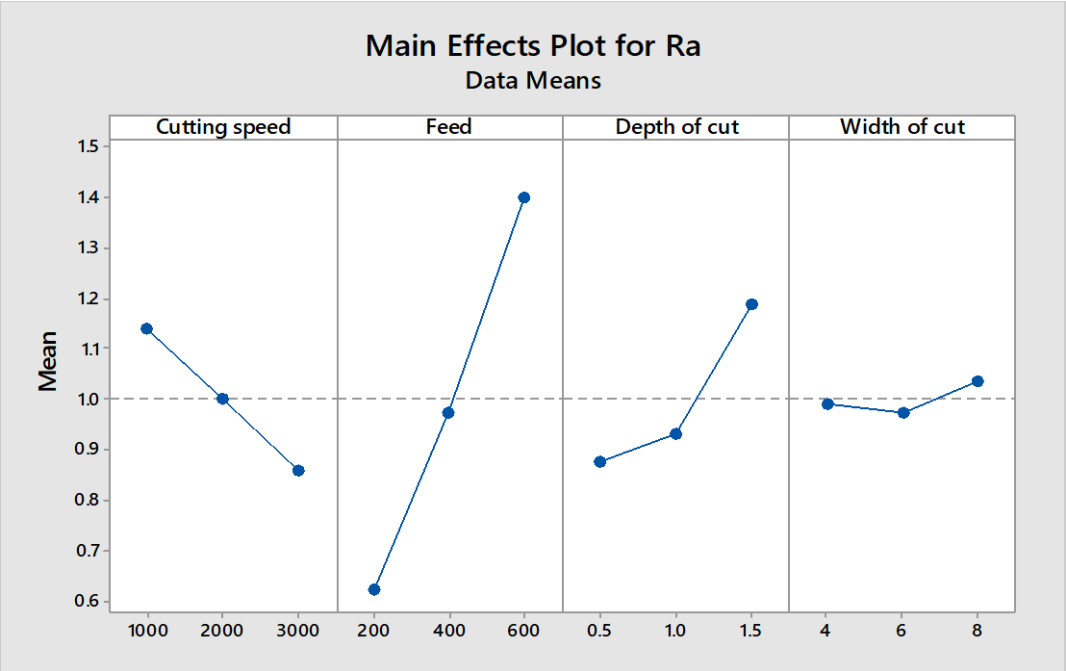

Figure 4.33 Main effect plot for surface roughness during wet cutting

Figure 4.34 Interaction plot for surface roughness during wet cutting

4.5.3 Predictive Modelling for Carbon Emissions

The predictive model for carbon emissions obtained using RSM, is as follows:

$$CE = 558.9 - 0.0191 * V_c - 0.7080 * f - 314.1 * a_p - 44.05 * a_e + 0.000004 * V_c * V_c + 0.000341 * f * f + 73.6 * a_p * a_p + 2.950 * a_e * a_e + 0.000007 * V_c * f + 0.02027 * V_c * a_p - 0.00372 * V_c * a_e + 0.1446 * f * a_p + 0.02336 * f * a_e \quad (4.11)$$

The values of carbon emissions for each experimental run were calculated using the predictive model and compared with the experimentally obtained values (Figure 4.35).

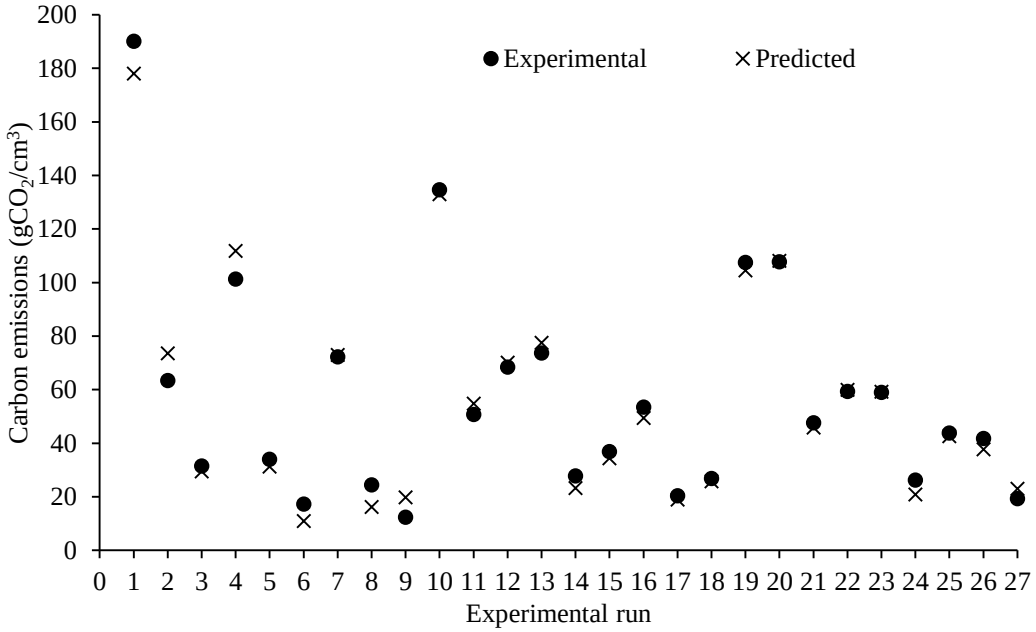

Figure 4.35 Experimentally measured and predicted values of carbon emissions during wet cutting

It was observed that the predicted values of carbon emissions were close to the experimentally measured values. The mean relative error between the experimental and predictive values was 11%. The relative importance of each process parameter, their interaction effect on CE and the adequacy of the model was tested using ANOVA with 95% confidence level and 5% significance level. Table 4.12 shows the ANOVA results for CE during wet experimental runs.

Table 4.12 ANOVA results for carbon emissions during wet cutting

Source	DF	Adj SS	Adj MS	F-Value	P-Value	% contribution	Remarks
Model	13	43101	3315.5	63.81	0	98.46	
Linear	4	28485	7121.4	137.05	0	65.07	
V_c	1	66	66.1	1.27	0.28	0.15	
f	1	13194	13194.1	253.92	0	30.14	$F^{standard}_{(0.05,13,26)}$=2.11
a_p	1	10560	10560.9	203.25	0	24.12	
a_e	1	1635	1635.2	31.47	0	3.74	$F^{regression} > F^{standard}_{(0.05,13,26)}$
Square	4	3154	788.6	15.18	0	7.21	
$V_c \times V_c$	1	99	99.2	1.91	0.19	0.23	
f × f	1	1118	1118.1	21.52	0	2.55	
$a_p \times a_p$	1	1524	1524.6	29.34	0	3.48	model is adequate
$a_e \times a_e$	1	626	626.7	12.06	0.004	1.43	
2-Way Interaction	5	4079	815.9	15.7	0	9.32	
$V_c \times f$	1	26	26.4	0.51	0.488	0.06	
$V_c \times a_p$	1	462	462	8.89	0.011	1.06	
$V_c \times a_e$	1	248	248.7	4.79	0.048	0.57	
$f \times a_p$	1	2509	2509.7	48.3	0	5.73	
$f \times a_e$	1	1047	1047.9	20.17	0.001	2.39	
Error	13	675	52			1.54	
Total	26	43777				100.00	
R^2 = 98.46%	R^2 (adj.) = 96.91%			R^2 (pred.) = 92.14%			

DF: Degree of freedom, SS: Sum of square, MS: Mean square

The tabulated F-value of the model at 95% confidence level was obtained to be 2.11. The model F-value (63.81) is higher than the standard tabulated value, which indicates the adequacy of the prediction model. It was also observed that the feed and depth of cut had the highest impact on carbon emissions with a percentage contribution of 30.14% and 24.12%, respectively. The value of R^2 was 0.9846 indicating that 98.46% of the total variance in the data can be explained by the model. R^2 (Adj.) was 0.9691 and R^2 (Pred.)

was 0.9214, which indicated a very good correlation. The residual plots were also analyzed to check the model adequacy (Figures 4.36 and 4.37). Both the figures indicate that the predictive model is adequate for the prediction of carbon emissions under dry cutting conditions.

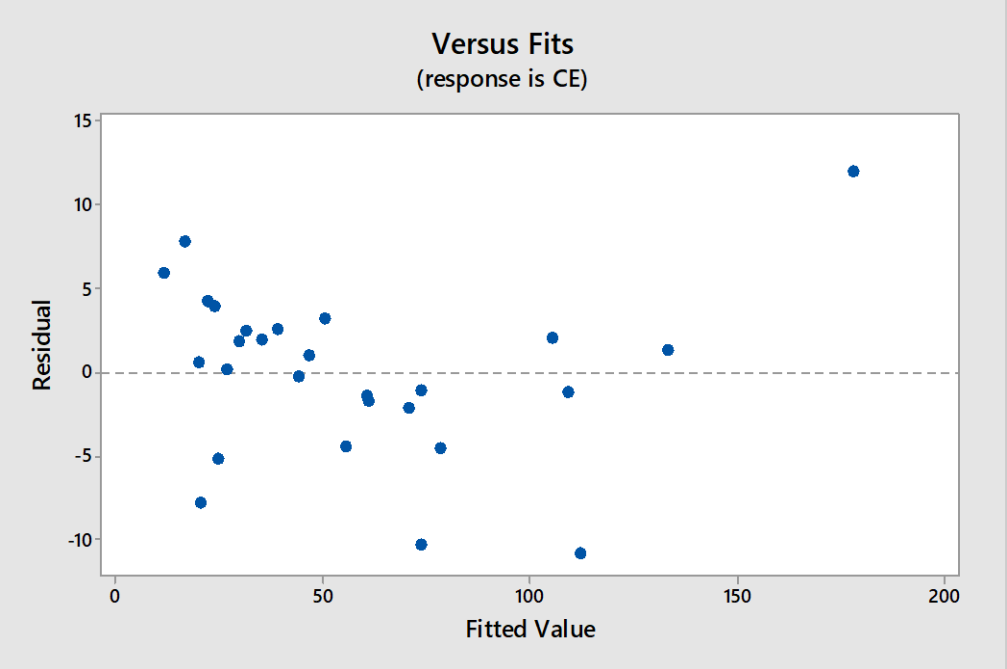

Figure 4.36 Residual v/s fitted value plot for carbon emissions during wet cutting

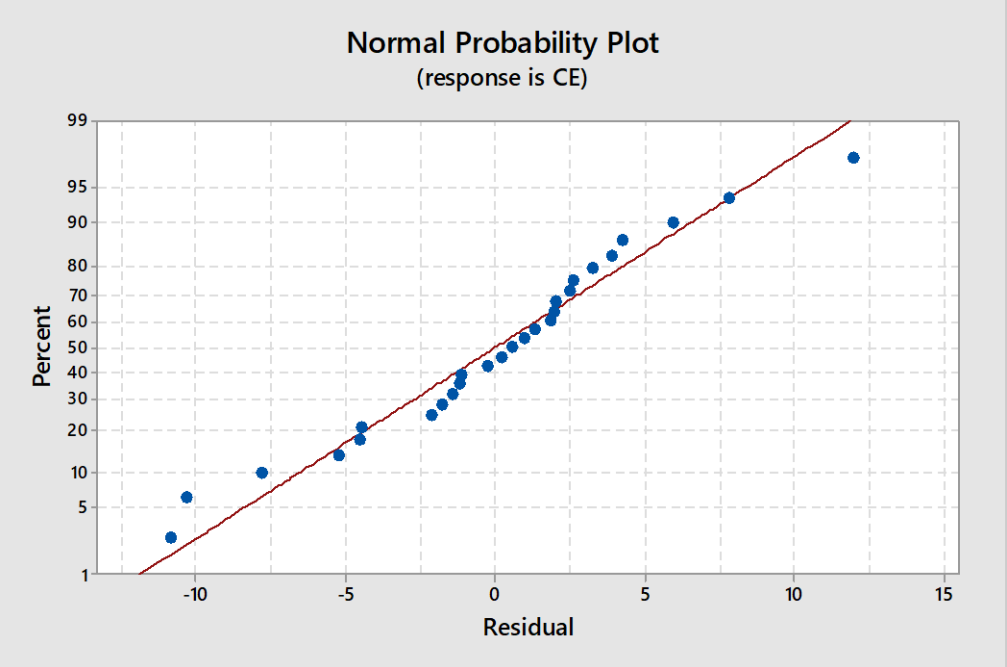

Figure 4.37 Normal probability plot of residuals for carbon emissions during wet cutting

The main effect and interaction plots for CE are shown in Figures 4.38 and 4.39, respectively. The carbon emissions due to energy, coolant consumption and disposal were considered here as explained in section 4.2.1.

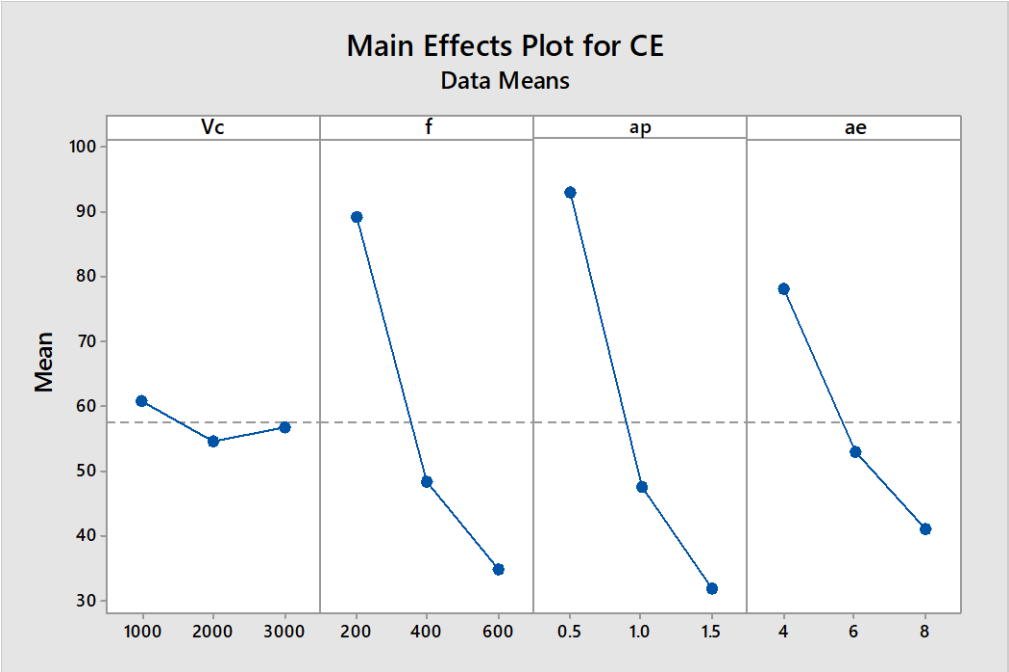

Figure 4.38 Main effect plot for carbon emissions during wet cutting

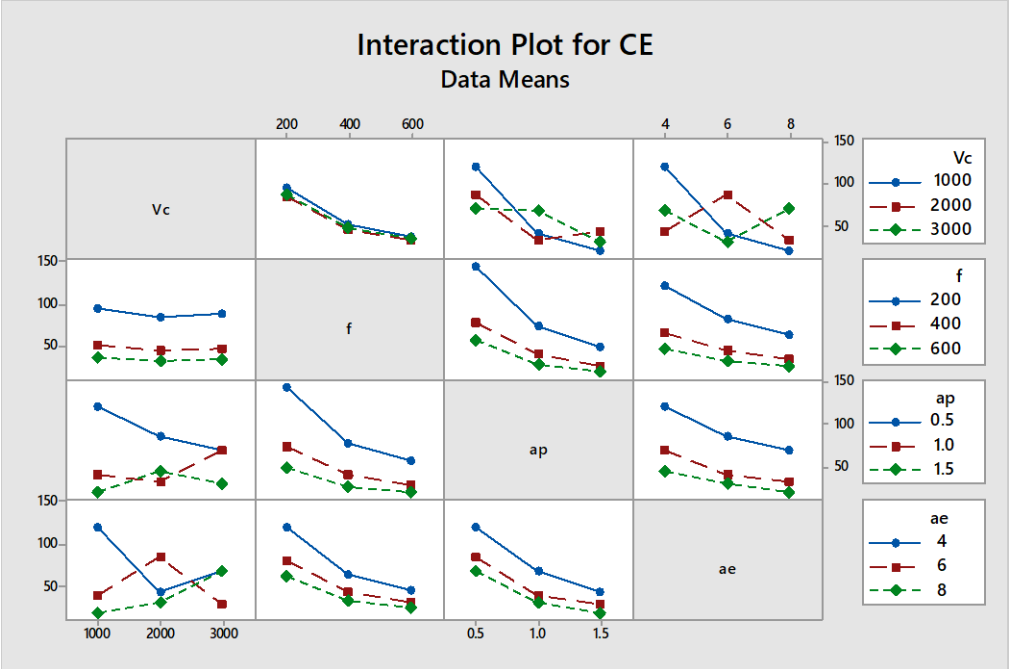

Figure 4.39 Interaction plot for carbon emissions during wet cutting

It is observed from Figure 4.38 that during wet cutting, the carbon emissions reduce with increase in feed, depth of cut and width of cut. This is because the material removal rate increases at higher cutting parameters, the processing time reduces; hence, the coolant consumption also reduces. However, the energy consumption is higher at higher cutting speed. The reduction in carbon emissions due to lower processing time is compensated by the increase in CE due to higher energy consumption. Therefore, the cutting speed has less effect on CE during wet cutting conditions.

4.6 MULTI-OBJECTIVE OPTIMIZATION OF PROCESS PARAMETERS

In this section, multi-objective optimization was performed to minimize the specific energy consumption and carbon emissions while targeting the surface roughness for pre-defined values. In the present study, the surface roughness was given five different target values and the optimization was conducted for five cases as follows:

Case 1: Minimize R_a, SEC and CE

Case 2: Target R_a = 0.5 μm and minimize SEC & CE

Case 3: Target R_a = 1 μm and minimize SEC & CE

Case 4: Target R_a = 1.5 μm and minimize SEC & CE

Case 5: Target R_a = 2 μm and minimize SEC & CE

4.6.1 Multi-objective Optimization using Desirability Approach

The cutting parameters were optimized using desirability approach and the optimization plots for the five cases are shown below (Figures 4.40-4.44). The optimization results based on desirability approach are provided in Table 4.13.

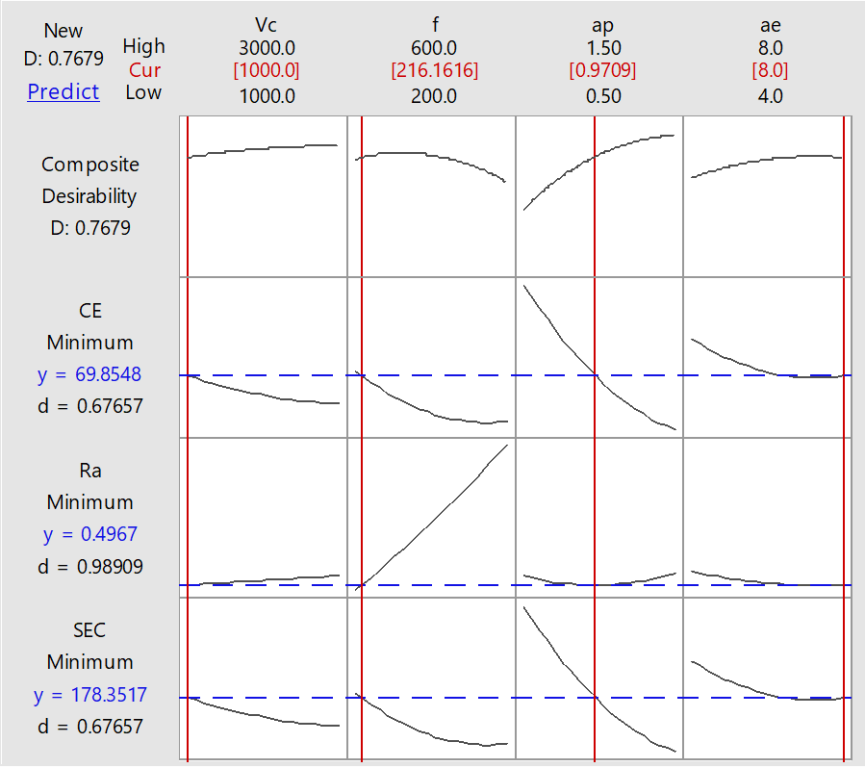

Figure 4.40 Optimization plot for case 1 (Minimization of R_a) during wet cutting

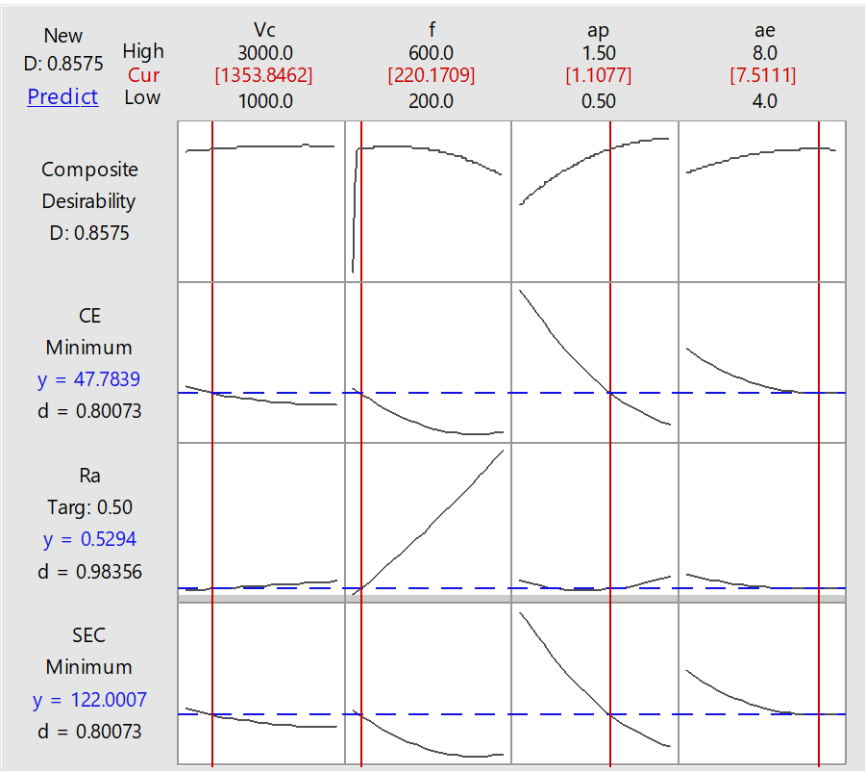

Figure 4.41 Optimization plot for case 2 (Target R_a = 0.5 µm) during wet cutting

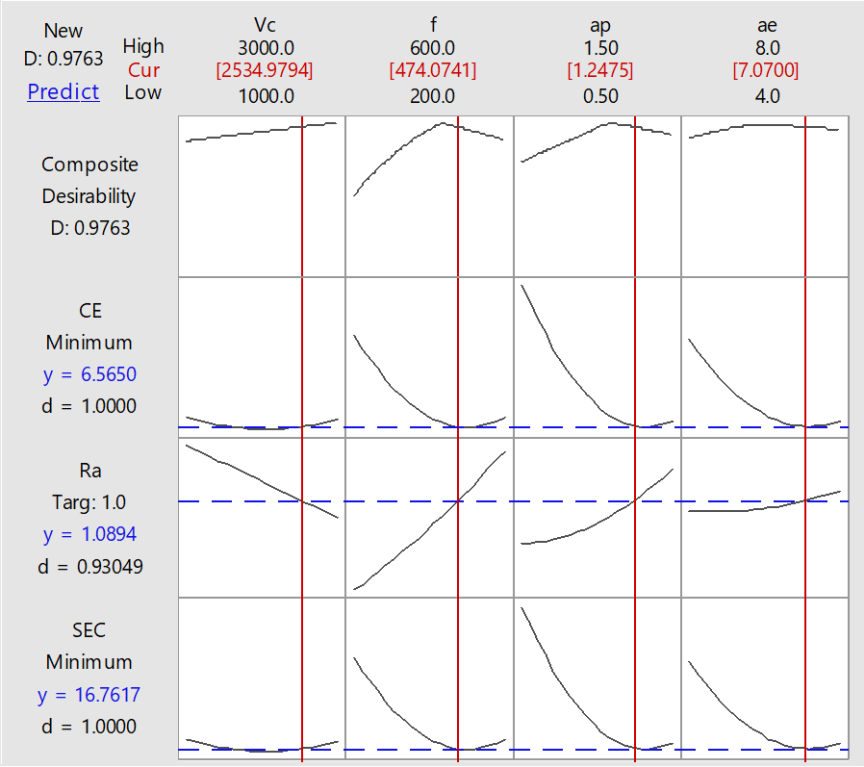

Figure 4.42 Optimization plot for case 3 (Target R_a = 1 µm) during wet cutting

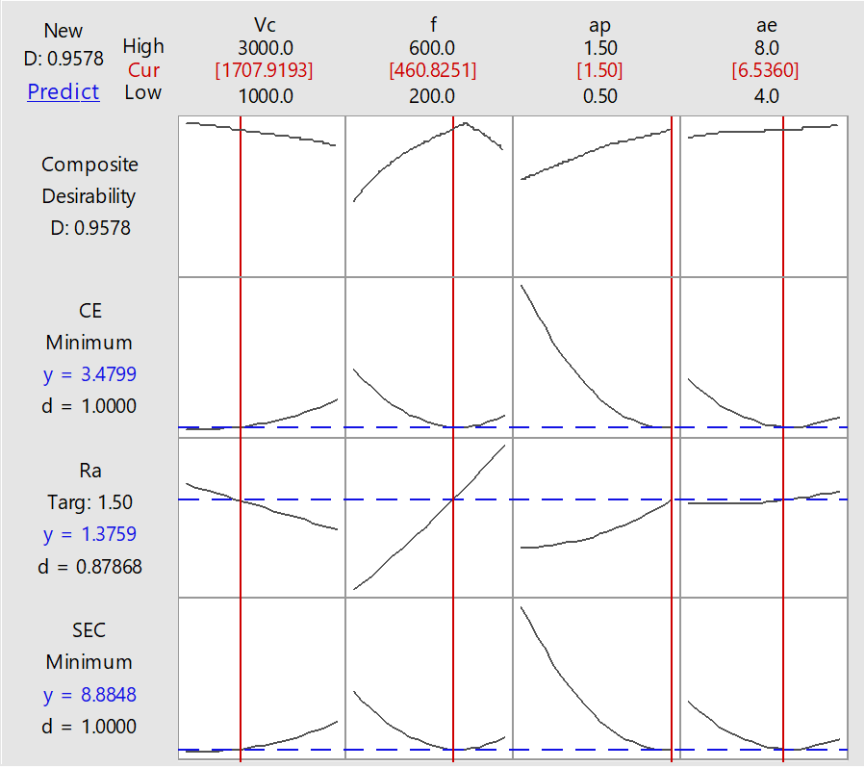

Figure 4.43 Optimization plot for case 4 (Target R_a = 1.5 µm) during wet cutting

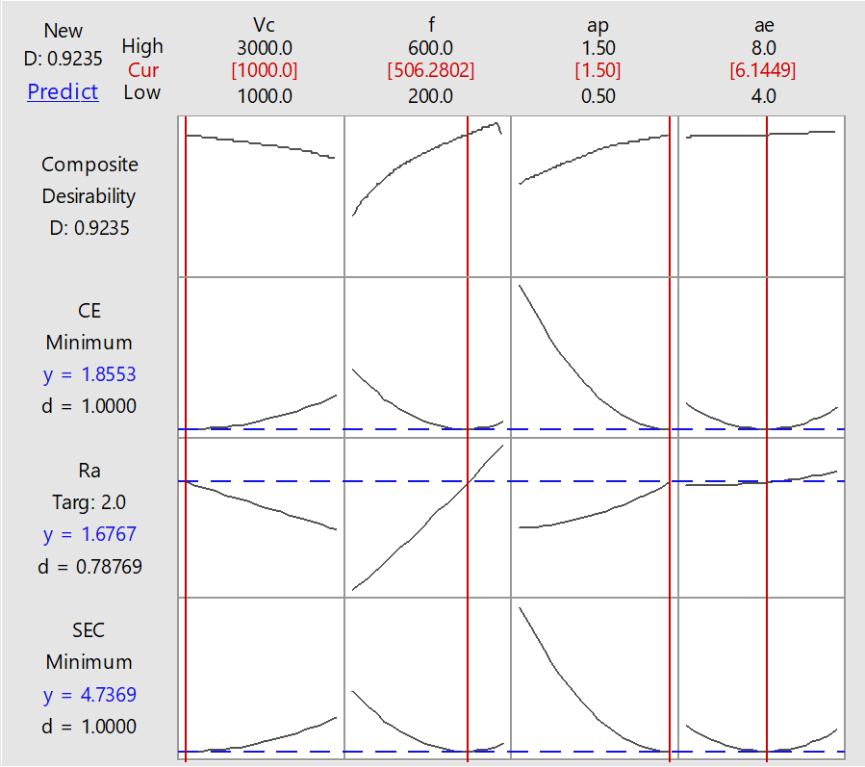

Figure 4.44 Optimization plot for case 5 (Target R_a = 2 µm) during wet cutting

Table 4.13 Multi-objective optimization results (wet cutting) using desirability approach

	V_c (RPM)	f (mm/rev)	a_p (mm)	a_e (mm)	R_a (µm)	SEC (J/mm^3)	CE (gCO_2/cm^3)
Case 1 (Minimization of R_a)	1000	216	0.97	8	0.496	178.35	69.85
Case 2 (Target R_a = 0.5)	1353	220	1.10	7.51	0.529	122.00	47.78
Case 3 (Target R_a = 1)	2534	474	1.25	7.07	1.089	16.76	6.56
Case 4 (Target R_a = 1.5)	1707	460	1. 5	6.53	1.376	8.88	3.47
Case 5 (Target R_a = 2)	1000	506	1.5	5.90	1.951	4.98	1.95

4.6.2 Multi-objective Optimization using MOGA

In the present study, multi-objective optimization was also performed using multi-objective genetic algorithm in MATLAB15 software. It was observed that the optimization result for case 2 converged towards the solution for case 1, because the target surface roughness value in case 2 is very less. The pareto charts for cases 3 – 5 are given in Figure 4.45. The optimization results are shown in Table 4.14.

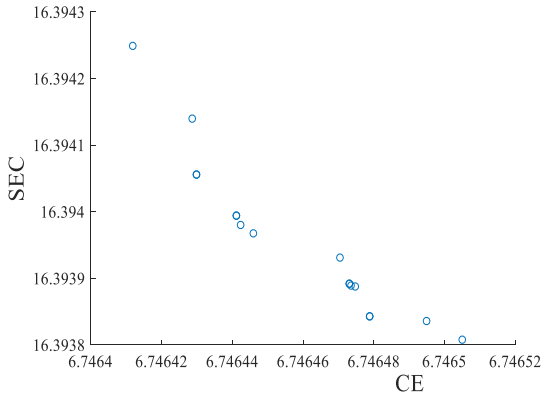

(a) Pareto chart (Target R_a = 1 µm)

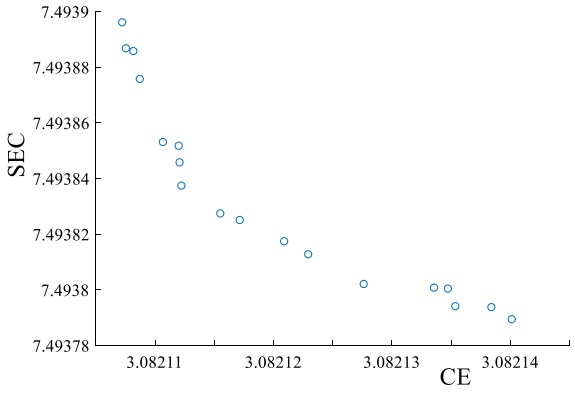

(b) Pareto chart (Target R_a = 1.5 µm)

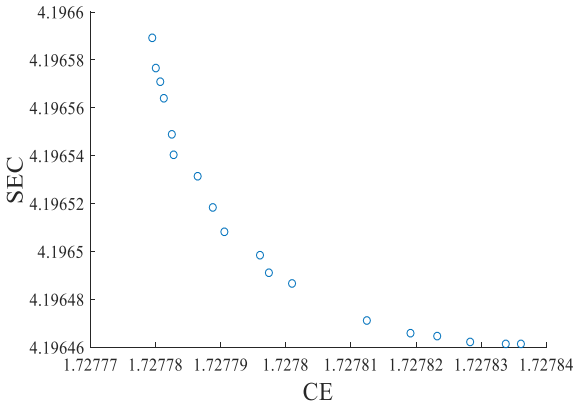

(c) Pareto chart (Target R_a = 2 µm)

Figure 4.45 Pareto charts for multi-objective optimization using MOGA during wet cutting

Table 4.14 Multi-objective optimization results (wet cutting) using MOGA

	V_c (RPM)	**f (mm/rev)**	**a_p (mm)**	**a_e (mm)**	**R_a (µm)**	**SEC (J/mm^3)**	**CE (gCO_2/cm^3)**
Case 1 (Minimization of R_a)	1358	204	1	7.5	0.479	160.98	63.29
Case 2 (Target R_a = 0.5)	1233	207	1.2	7.3	0.501	112.56	44.30
Case 3 (Target R_a = 1)	2529	421	1.3	7.2	1.006	16.39	6.75
Case 4 (Target R_a = 1.5)	2011	497	1.4	6.8	1.345	7.49	3.08
Case 5 (Target R_a = 2)	1372	494	1.5	6.4	1.545	4.20	1.73

4.7 DISCUSSION

The variation in the three process responses – SEC, CE and surface roughness was analyzed with respect to the machining parameters of cutting speed, feed, depth of cut, and width of cut. During dry cutting conditions, it was observed that the carbon emissions

increased with cutting speed. At lower cutting speed range, the SEC is less influenced by cutting speed, but after a certain value, it starts to increase with cutting speed. Therefore, lower cutting speed is preferred to reduce CE and SEC. But lower cutting speed results into high surface roughness. Therefore, higher cutting speed is to be used for minimization of surface roughness, compromising the carbon emissions and SEC. When the target surface roughness is increased, lower cutting speed can be used for machining, leading to lesser SEC and CE. With increase in feed, SEC reduces and surface roughness increases. For minimization of surface roughness, lower feed rate is to be selected. But as the target value for surface roughness increases, higher feed rates can be selected leading to lower SEC. Increase in depth of cut reduced all the three responses; therefore, high depth of cut is preferred for multi-objective optimization. Increase in width of cut reduces SEC and CE. However, the surface roughness first increases and then decreases with width of cut.

The optimum machining parameters and corresponding process responses for the five different target surface roughness values are presented in Tables 4.8 and 4.9. It is evident here that a slight increase in surface roughness can lead to significant reduction in SEC and CE for the machining process.

The second set of experimentation was conducted at the same machining parameters but with coolant. It is observed that, the surface roughness reduces with increase in cutting speed. The SEC and CE, reduces with increase in cutting speed initially and then starts to increase after a certain value of cutting speed. For minimization of surface roughness, higher cutting speed is selected which increases the SEC and CE for the machining process. As the target surface roughness is increased, it allows for the selection of lower cutting speeds, which reduce the SEC and CE. Similarly, as the depth of cut increased, the SEC and CE reduces but surface roughness increases. Higher depth of cut cannot be selected for minimization of surface roughness. However, when the target surface

roughness is increased, selection of higher depth of cut is allowed and the SEC and CE can be reduced. The optimum machining parameters and corresponding process responses with coolant application for the five different cases are presented in Tables 4.13 and 4.14. The results show that slight increase in surface roughness can result into significant reduction in SEC and CE. Therefore, minimization of surface roughness is not the most practical approach and the research should focus on achieving the design specified surface finish while improving the energy and carbon efficiencies.

4.8 SUMMARY

In this chapter, the machining parameters were optimized for minimization of SEC and CE while achieving the required surface finish. The range of machining parameters was selected based on the recommendation from the tool manufacturer, workpiece properties and the parameters used in the existing literature. The experiments were designed using Taguchi's L_{27} orthogonal array. The experiments were conducted as per the design of experiments and the process responses were obtained for each experimental run. Two set of experiments were conducted under different coolant conditions – dry and wet cutting. The predictive models for the three responses – SEC, CE and surface roughness were obtained for both cases by using response surface methodology (RSM). The adequacy of the models and their fitness was tested using statistical analysis. Then, multi-objective optimization was performed using two approaches – desirability analysis and multi-objective genetic algorithm. It was observed that significant reduction in SEC and CE can be achieved with optimization of cutting parameters. In addition, minimization of surface roughness requires higher SEC and causes more CE for the machining process. Therefore, a more practical approach is to target the surface roughness for a pre-defined value provided by the designer.